République Algérienne Démocratique et Populaire
Ministère de l'Enseignement Supérieur et de la Recherche Scientifique
Université A. MIRA-BEJAIA

جامعة بجاية
Tasdawit n Bgayet
Université de Béjaïa

Faculté de Technologie
Département de Génie Electrique
Laboratoire de Technologie Industrielle et de l'Information (LTII)

THÈSE

EN VUE DE L'OBTENTION DU TITRE DE

DOCTEUR

Domaine : Science et Technologies, Filière : Electronique
Spécialité : Electronique

Présentée par

BELKHIER Youcef

Thème

CONTRIBUTION TO THE ADVANCED CONTROL STRATEGIES OF A TIDAL TURBINE GENERATOR CONVERSION SYSTEM

Soutenue le : 03/06/2021 **Devant le Jury composé de :**

Nom et Prénom		Grade		
Mr	**MENDIL Boubekeur**	**Professeur**	Université A/Mira de Béjaia	Président
Mr	**ACHOUR Abdelyazid**	**MCA**	Université A/Mira de Béjaia	Rapporteur
Mr	**HAMOUDI Farid**	**MCA**	Université A/Mira de Béjaia	Examinateur
Mr	**MOHAMMEDI Ahmed**	**MCA**	Université de Bouira.	Examinateur
Mme	**BOUZIDA Radia**	**MCA**	Université A/Mira de Béjaia	Examinateur

Année Universitaire : 2020/2021

List of Publications

Main results of this PhD thesis have lead to the following publications

International Journal Papers

[1] **Belkhier Y**, Achour AY. An intelligent passivity-based backstepping approach for optimal control for grid-connecting permanent magnet synchronous generator-based tidal conversion system. *International Journal of Energy Research*, 2020: 1-16, 2020. DOI: 10.1002/er.6171.

[2] **Belkhier Y**, Achour AY. Passivity-based voltage controller for tidal energy conversion system with permanent magnet synchronous generator. *International Journal of Control, Automation and Systems*, 2020; 19: 1-11. http://dx.doi.org/10.1007/s12555-019-0938-z.

[3] **Belkhier Y**, Achour AY. Fuzzy passivity-based linear feedback current controller approach for PMSG-based tidal turbine. *Ocean Engineering*, 2020; 218: 108156. https://doi.org/10.1016/j.oceaneng.2020.108156

[4] **Belkhier Y**, Achour AY, Ullah N, Shaw RN. Modified passivity-based current controller design of permanent magnet synchronous generator for wind conversion system. *International Journal of Modelling and Simulation*, 2020. DOI: 10.1080/02286203.2020.1858226.

[5] **Belkhier Y**, Achour AY, Hamoudi F, Ullah N, Mendil B. Robust energy-based nonlinear observer and voltage control for grid-connected permanent magnet synchronous generator in the tidal energy conversion system. *International Journal of Energy Research*, 2021;1-19. DOI : 10.1002/er.6650.

[6] **Belkhier Y**, Achour AY, Shaw RN, Ullah N, Chowdhury MDS, Techato K. Energy-based combined nonlinear observer and voltage controller for a PMSG using fuzzy supervisor high order sliding mode in a marine current power system. *Sustainability*, 2021; 13(7): 3737. DOI: 10.3390/su13073737.

[7] **Belkhier Y**, Achour AY, Ullah N, Shaw RN, Farooq Z, Ullah A, Ali NA. Intelligent energy-eased modified super twisting algorithm and factional order PID control for performance improvement of PMSG dedicated to tidal Power System. *IEEE Access*, 2021: 1-12. DOI: 10.1109/ACCESS.2021.3072332.

[8] **Belkhier Y**, Achour AY, Shaw RN, Ullah N, Chowdhury MDS, Techato K. Fuzzy supervisory passivity-based high order-sliding mode control approach for tidal turbine-based permanent magnet synchronous generator conversion system. *Actuators*, 2021. Accepted for Publication on 22/04/2021.

International Conference Papers

[1] **Belkhier Y**, Achour AY, Shaw RN: Fuzzy passivity-based voltage controller strategy of grid-connected PMSG-based wind renewable energy system. *In: 2020 IEEE 5th International Conference on Computing Communication and Automation (ICCCA)*, pp. 210-214, Greater Noida, India (2020). DOI: 10.1109/ICCCA49541.2020.9250838.

[2] **Belkhier Y**, Achour AY: Passivity-based current control strategy for PMSG wind turbine. *In: 2019 IEEE 1st International Conference on Sustainable Renewable Energy Systems and Applications (ICSRESA)*, pp. 1-4, Tebessa, Algeria (2019). DOI: 10.1109/ICSRESA49121.2019.9182518.

[3] **Belkhier Y**, Achour AY, Shaw RN. An Intelligent Passivity-Based Control for Tidal Power Conversion System with PMSG. *2020 International Conference on Data Analytics for Business and Industry: Way Towards a Sustainable Economy (ICDABI)*, Sakheer, Bahrain. DOI: 10.1109/ICDABI51230.2020.9325666

[4] **Belkhier Y**, Achour AY, Shaw RN. Passivity-Based Linear Feedback Current Controller of Wind Conversion System Based Permanent Magnet Synchronous Generator. *2020 Seventh International Conference on Information Technology Trends (ITT)*, Abu Dhabi, United Arab Emirates. DOI: 10.1109/ITT51279.2020.9320868.

[5] **Belkhier Y**, Achour AY. Passivity-Based Voltage Control Design of Grid Connected Wind Turbine With PMSG. *2020 IEEE ANDESCON*, Quito, Ecuador. DOI: 10.1109/ANDESCON50619.2020.9272189.

Acknowledgement

First of all, I thank God Almighty *'Allah'* for keeping me alive and allowing me to complete this doctoral thesis. Without Him none of this would have existed.

I would like to thank my main supervisor *Dr. Abdelyazid ACHOUR* for his continuous support, guidance and valuable correction suggestion throughout my dissertation over the past three years, who is always available to discuss technical issues, to provided great ideas and to contribute the possible solutions. I am really appreciated everything he has done for me in this PhD thesis. His life philosophy and serious research attitude will influence all my life.

I am grateful to the honored pre-examiners of the dissertation, *Prof. Boubekeur MENDIL* from, *Dr. Farid HAMOUDI*, *Dr. Radia BOUZIDA* from University of Bejaia and *Dr. Ahmed MOHAMMEDI* from University of Bouira for accepting to be a member of the jury.

Last, but definitely not least, I would like to thank my lovely wife, Zahra MADJI, for her support and to live with me during this thesis. Without her love, continual support and patience this project would not have been possible finished, who gives me illimitable motivation to finish this thesis. I also would like to thank my parents Hemanou BELKHIER and Nadia MOHADEB for showing and teaching me man should work harder to make a better life for his family. Thanks, are also given to my dear parents in-law, Abdennour MADJI and Khelidja AZIRI, for their endeavors help and support.

Summary

Table of Contents

Chapter IV: Fuzzy passivity-based linear feedback current controller approach for PMSG-based tidal turbine

Chapter V: An intelligent passivity-based backstepping approach for optimal control for grid-connecting permanent magnet synchronous generator-based tidal conversion system

Conclusions

Appendix

Table of Figures

Introduction

Global energy necessities are essentially given by the burning of fossil fuels. The result of this overwhelming reliance is turning into an expanding worry because fossil fuels have restricted potential [1]. Because of the present rate of misuse, these assets will exhaust in the coming decades. The CO2 discharged from the conventional energy sources into the air from these fuels fills limits the earth from emanating the warmth from the sun once again into space, bringing about an ascent in worldwide temperature. Sustainable power sources that are normally renewed are those created from regular assets, for example, wind, sunlight, tidal, hydro, biomass, geothermal, and sea sources, has been growing rapidly during the recent years [2].

Tidal power, additionally called tidal energy, is a type of hydropower that changes the energy of tides into power or other valuable types of energy. Despite the fact that it is not yet broadly utilized, tidal power has the potential for a future power era. Tides are more unsurprising than wind energy and sun-based power [3]. Among wellsprings of renewable power sources, tidal power has customarily experienced moderately high cost and constrained accessibility of destinations with adequately high tidal ranges or stream speeds, hence chocking its aggregate accessibility. The exploitable marine current power with present technologies is estimated about 75 GW in the world. The kinetic energy available in tidal currents can be converted to electricity using relatively mature turbine technologies called “Tidal turbine or marine current turbine”. However, there are still some difficulties before commercialization of the marine current turbine system. On the one hand, the installation cost, geographical constraints and social acceptance should be considered in planning the marine current turbine projects [4].

The aim of this *Ph.D.* thesis is to investigate the transformation of the tidal power to electrical power using tidal turbine conversion system and some control strategies are developed to improve the harnessed power quality and energy management capability. The contribution of this thesis can be summarized as follows:

- A tidal conversion system-based permanent magnet synchronous generator (PMSG) is simulated under Matalab/Simulink platform and investigated which is constituted by a tidal turbine, PMSG, power converters and grid-connection.
- Original control strategies based on an energy approach are proposed to improve the power quality harnessed by the PMSG-based tidal conversion system.

The rest of this thesis is organized in chapiters as follow:

Chapter I presents the review of tidal power generation and power plant, developments in large marine current turbine technologies are summarized, it gives the state of the art of tidal energy systems: issues, challenges and possible solutions.

Chapter II proposes an up-to-day and review on the passivity theory.

Chapter III proposes a new control strategy based on passivity principe for a grid-connected tidal turbine-based PMSG conversion system.

Chapter IV deals with a fuzzy passivity-based current controller with a linear feedback to improve the performances of the conversion system based on the flux orientation of the PMSG.

Chapter V presents an original controller which is inspired from the aforementioned controls associated to backstepping method with adaptation of the PMSG stator resistance, that improve the robustness, stability and power generation quality.

Chapter I

Current Statues in Tidal Power Technologies

1 Introduction

There is worldwide agreement on the need to reduce greenhouse gas emissions, and different policies are evolving both internationally and locally to achieve this. This kind of world trend drives people to explore different kinds of renewable energy such as wind power, solar power and ocean power. More and more organizations, companies and laboratories start to focus on exploring ocean power [1]. More than 70% of the earth area is covered by ocean and in which stored a vast of energy. The existed various forms in ocean power are namely tidal rise & fall energy, tidal (ocean) current energy, wave energy, salinity gradient and thermal gradient energy. Among them, tidal current energy has obtained a strong increasing interest due to the advantages of predictable, high power density and huge potential characteristics in the last decade [2]. However, the maximum power which can be extracted is nonlinear, due to the water flow speed, also a tidal system based PMSG can capture significantly more power than a wind system with the same characteristic due to the water density which is thousand times higher than the air density. In this chapter, a review and state of the art of tidal energy storage technologies are presented [3].

2 Tidal Energy Technologies Review

There are two fundamentally different approaches to exploiting tidal energy. The first is to exploit the cyclic rise and fall of sea levels using barrages where energy is extracted from the potential head of the water similar to a hydropower generation. The second is to harness local tidal currents in a manner somewhat analogous to wind power. This method extracts the kinetic energy of the moving water by means of tidal current energy converters such as tidal turbines [1].

In contrast, tidal current turbines, or also referred as tidal stream turbine, are designed to generate electricity by directly converting the kinetic energy from the marine current. It resembles more closely wind turbines in that they directly harness the kinetic energy of the water flow using individual units, rather than the tidal barrages that block entire water channels in order to utilize potential energy to funnel water into their generators. For this reason, tidal current turbines are significantly less detrimental towards the environment (Figure I.1) [4].

Generating energy from tidal current turbines are less environmentally invasive too as compared to tidal barrages generation. As water is much denser than air, tidal current turbines do not need to run at excessive speeds to produce reasonable amount of energy [5]. Due to the same reason, tidal

current turbines are also smaller in size as they do not require large blade to capture as much energy as a wind turbine would as the water is thousand time denser than air. Similarly, the hydrodynamic forces subjected on the tidal current devices are higher requiring them to be more robust. Various tidal current energy converters have been developed, diverting from the traditional concept of extracting tidal energy using tidal barrages [6].

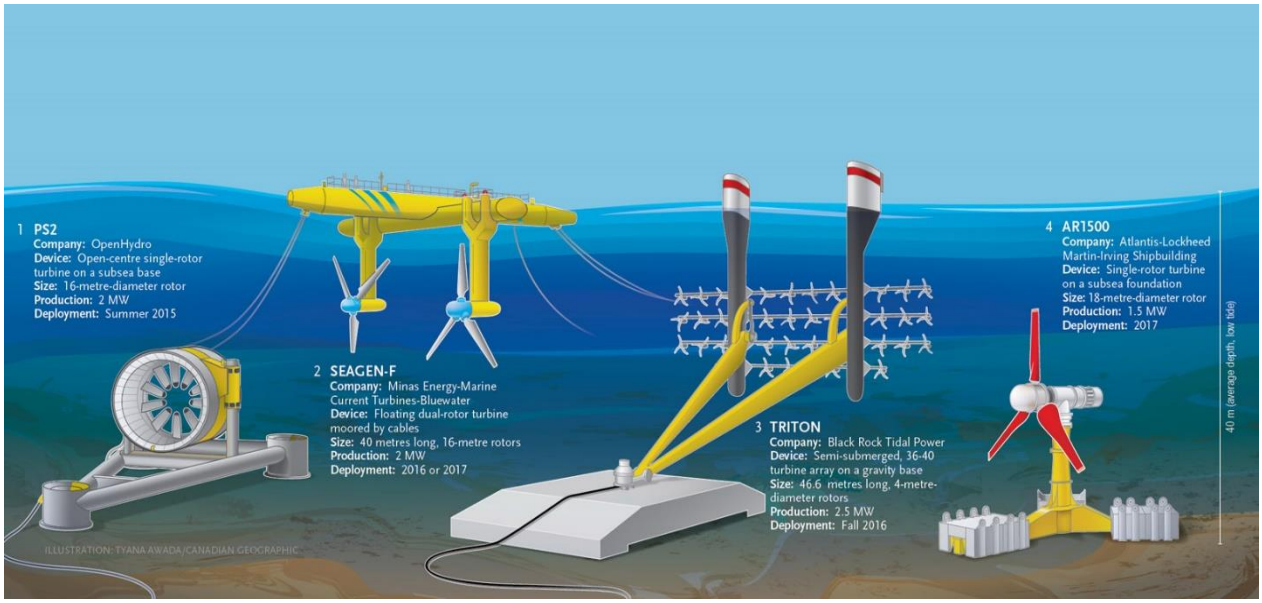

FIGURE I.1 Tidal energy turbines.

There are two types of tidal current turbines. One is the horizontal axis turbines and the other is the vertical axis turbines. Horizontal axis turbines rotate around an axis parallel to the waterflow, and vertical axis turbines rotate around an axis perpendicular to the waterflow. Both types of turbines consist of a group of blades attached to a rotor, which ultimately connects to a generator. As the water passes through the turbine, the rotor uses the blades to rotate, and this kinetic motion is then converted to electric energy, which is stored in the generator. The configuration of the blades themselves has been varied from design to design, as researchers try to find the most efficient pattern that could generate the most electricity with the least amount of kinetic energy [1].

The power generation that can be exploited with tidal current technologies is assessed to be around 75 GW worldwide, 11 GW in Europe especially in UK (6 GW) and France (3.4 GW). Numerous researches have been carried out on TCT in recent years but these studies are still in the experimental phase in diverse sites. In a recent survey, some researchers had listed the companies that have started establishing tidal current turbine farms such as Andritz Hydro Hammerfest (AHH) in Anglesey (Wales, UK), Sabella in France, GE & Alstom Energy (France), MeyGen in Scotland,

GE & Alstom Energy, and DCNS, EDF (France & Canada) which will start working in following years. The French industrial group DCNS and French electric utility company EDF have chosen to build a first demonstrative marine current turbine (MCT) farm off the coast of Paimpol-Bréhat in Brittany, France at European Marine Energy Center (EMEC) off Orkney Islands in Scotland (namely "OpenHydro turbine"). The first 500 kW OpenHydro turbine (Figure I.2) was tested in September 2011 near Brest, France. This 850 t turbine has a diameter of 16 m and is supposed to be installed at a depth of 35 m. This technology uses multi-blades fixed between the open-center rim and the outside shell in a rim-driven configuration. A permanent magnet synchronous generator (PMSG) is integrated into the rim shell. Andritz Hydro Hammerfest, pre- commercialezed the 1 MW turbine HS1000 (showed in Figure I.3) at EMEC tidal test site at the end of 2011. It started delivering energy to the grid in 2012 [1], [5].

FIGURE I.2 500 kW OpenHydro turbine.

FIGURE I.3 Atlantis AR1500 turbine.

Atlantis Resources Corporation hes been tested the MeyGen project is AR1500 turbine (showed in Figure I.4) at the EMEC facility during the summer of 2011. This 1 MW turbine adopts fixed pitch configuration and reaches its rated power at a current velocity of 2.65 m/s. A yaw drive mechanism enables the turbine to face the tide when the tidal flow changes direction, which is is now under development for future turbine farm installation in the Pentland Firth in Scotland and the Bay of Fundy in Canada. The 1 MW pre-commercial turbine HS1000 (showed in Figure I.4) was tested by Andritz Hydro Hammerfest at EMEC tidal test site at the end of 2011. It started delivering energy to the grid in 2012. The HS1000 turbine technology uses advanced composite blades consisting of glass and carbon fiber for enduring severe seawater environment. The blades can be pitched for two-direction current flows [1], [6], [7].

FIGURE I.4 The HS1000 turbine technology.

Acquired by Atlantis Resources in April 2015, the 1.2 MW SeaGen S (2×600 kW) turbine (showed in Figure I.5) developed by Marine Current Turbine Ltd, is the world first grid-connected megawatt-level MCT system. It was installed in Strangford Lough in Northern Ireland in 2008 and has

FIGUER I.5 SeaGen S (2×600 kW) turbin.

FIGURE I.6 Voith Hydro turbine system.

Another candidate, is the Voith Hydro turbine system (shown in Figure I.6) developed by German hydropower equipment maker Voith Company. It uses fixed-pitch blades and direct-drive PMSG to achieve compact structure. The first test turbine of 110 kW has been in operation near

the South Korean island of Jindo since 2011. The up-scaled version of 1 MW turbine is now installed and tested at EMEC tidal test site [1], [5-7].

3 Electricity Production From Marine Renewable Energies

For the installation of a tidal turbine, it is crucial to select the right site. This is why a good knowledge of the characteristics of marine currents is fundamental. There are two main types of currents. Global currents due to differences in temperature and salinity of nearby water masses. They can be divided into two categories : local currents linked to winds and regular currents such as the Gulf Stream. Another type of current consists of the so-called tidal (or tidal range) currents that are found near the coasts or at the mouths of rivers. These currents originate from the movement of the stars of the solar system. They result from the interaction of the earth, the moon and the sun and are directly related to the movement of water associated with the tides. Offshore, they are roundabout but turn into alternating currents in a preferred direction as they approach the coast. Tidal currents are generally accelerated according to the topography of the bottom, particularly around headlands, straits between islands and in shallow water areas. It is the latter that are of most interest to industrialists [3].

Some areas are of particular interest because their underwater topography allows high current speeds. Indeed, the extractable power depends on the cube of the velocity, which shows the interest of choosing sites with the highest possible velocities. For both technological and economic constraints, the minimum exploitable threshold value is currently established at 1 m/sec, i.e. about 2 nodes. This minimum threshold value is likely to be lowered as technology evolves. Nevertheless, to avoid possible additional costs, it is also necessary to consider the maximum current value which corresponds to the nominal power of the system and which is thus preponderant in the dimensioning of the installation [8].

The choice of the installation site for the tidal turbines is also made in relation to the depth of the seabed. The depth values of sites that have been identified as having exploitable currents are characterized by water depths between 30 and 40 m. It is also necessary to take into account the variations in levels and speed due to the swell and more generally to the sea state. It thus appears that among the different technologies proposed and studied up to now, some appear to be much more adapted to certain sites than to others depending on the nature of the current ellipse, the nature

of the seabed and the local bathymetry. The search for an optimal combination between a site and a technology therefore appears to be a multi-objective multi-criteria analysis [4], [8].

4 Tidal Conversion System Configuration Choices

4.1 Tidal Conversion System-based on Doubly Fed Induction Generator

The Doubly Fed Induction Generator (DFIG) is the most commonly used one for wind integration due to its high efficiency, fast reaction and robustness during faults. This type of generator (Figure I.7) is built out of a wound-rotor induction generator with its stator is directly connected to the grid, whereas the wound rotor is connected through a power electronic converter. The variable speed range is ±30% around the synchronous speed. The rating of the power electronic converter is only 25~30% of the generator capacity, which makes this concept attractive and popular from an economic point of view. However, DFIG is probably not the case in tidal turbine applications except in special cases comparing to PMSG direct drive system.

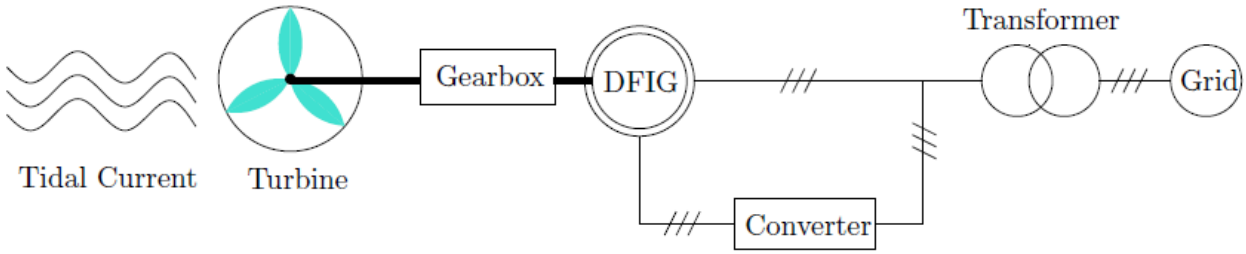

FIGURE I.7 Doubly Fed Induction Generator System Topology.

This method of generation was analyzed, implemented, and tested in using the linear version intended for Tidal generator applications.

4.2 Tidal Conversion System-based Permanente Magnet Synchronous Generator

The advantages of PMSG are compact structure, high efficiency, and the possibility to eliminate the gearbox. These characteristics lead to low maintenance requirement and enable the PMSG to be very favorable in underwater applications. Recent industrial tidal current projects have adopted the PMSG as the generator type in the tidal conversion system, for instance, the OpenHydro turbine system (proposed by French Electricity) and the Clean Current project (proposed by Alstom).

PMSG is normally used in direct drive train option with full scale power converter connect to the grid as Figure I.8 showed. PMSG system has high potential for the tidal current turbines because of its reduced failure, increased energy yield and reliability.

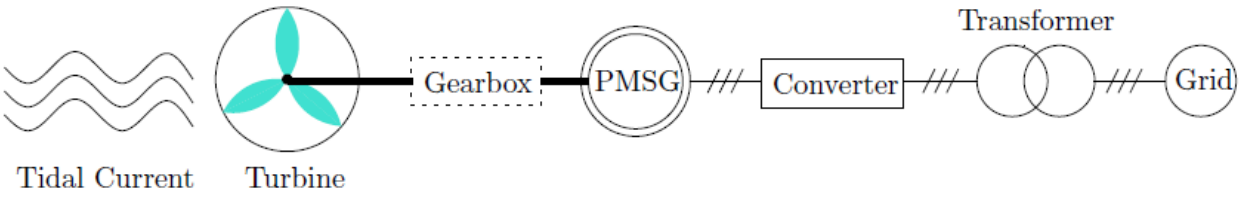

FIGURE I.8 Permanent Magnet Synchronous Generator System Topology.

Both gearbox or direct drive system now are using in the new energy market. However, in direct drive system, the low rotational speed characteristic leads to bigger pole pairs generator design and then leads to bigger system volume and mass. In order to reduce the size and mass of system, a gearbox can be introduced as the dotted line shown in Figure I.8. Especially for floating platform turbines, this seems to be the trend even that gearbox system needs high maintenance cost. For the direct-drive, particularly for the horizontal ducted turbines, PMSG are preferred [9].

5 Modeling of Tidal Energy Conversion Systems

5.1 Modeling of Tidal Power

The basic ideology applied to the pulling of hydrokinetic energy from the rated value of tidal currents at different tidal ranges is the same as those for wind and hydro energy systems. The power delivered in a moving fluid is a function of the mass flow rate, which is a measure of the mass of fluid passing a point in the system per unit time, it is working as the active element of the system. The output of mechanical power captured from the low and high tides by a tidal turbine can be formulated as

$$P_m = \frac{1}{2}\rho A v_t^3 \tag{I.1}$$

Where, v_t denotes the tidal speed, ρ represents water density, A represents the blades swept area [3].

This formula provides a computation of the amount of active power that could be extracted per unit area from a hydrokinetic resource if the given power from the tidal power plant could be extracted at 100% efficiency. It is a functional measure for determining the ability of the tidal resource. However, in practice a tidal turbine will only be able to extract a fraction of this available power. The above equation is modified to give the actual power that a tidal turbine is able to extract. This is given by the following equation

$$P_m = \frac{1}{2}\rho C_p(\beta,\lambda)Av_t^3 \quad (I.2)$$

Where, β denotes the pitch angle, λ denotes tip-speed ratio, C_p is a dimensionless term that describes the hydrodynamic efficiency of a turbine. The C_p value is a ratio between the actual power extracted by the rotor to the total kinetic energy incident over the cross-sectional area of the rotor

$$C_p(\beta,\lambda) = 0.5\left(\frac{116}{\lambda_i} - 0.4\beta - 5\right)e^{-\left(\frac{21}{\lambda_i}\right)} \quad (I.3)$$

$$\lambda_i^{-1} = (\lambda + 0.08\beta)^{-1} - 0.035(1+\beta^3)^{-1} \quad (I.4)$$

Due to the Betz limit, it is only possible to extract a total of 59.3% of the total kinetic energy available in the flow of tidal current. In addition, the conversion efficiency of hydrodynamic, mechanical, and electrical processes reduces the overall output further. So in practice, most real turbines have efficiencies that are lower than the Betz limit, with values in the range 0.4–0.5 for modern axial flow turbines [1, 4]. The tip speed ratio (TSR) is the ratio between the rotational velocity at the tip of the rotor blade and the flow speed, and is given by

$$\lambda = \frac{\omega_m R}{v_t} \quad (I.5)$$

Where ω_t is the rotational velocity of the rotor of the tidal turbine and R is the radius of the rotor of the tidal turbine. And torque developed by a tidal turbine can be expressed as

$$T_m = \frac{P_m}{\omega_m} \quad (I.6)$$

6 Modeling of Permanent Magnet Synchronous Generator

The synchronous machines (see Figure I.9) have many advantages over induction machines. One of them is a higher efficiency. It is because the magnetising current is not a part of the stator current. In induction machines reactive power for rotor excitation is carried by stator winding as well as the active power for conversion. Accordingly, synchronous generators (SGs) will have better efficiency and better power factor. In tidal systems, usually, the synchronous generators are connected to the grid via a power electronic converter. The amount of deliverable active power from Synchronous Generator depends on rating of a converter in Volt-Amperes and its power

factor. Thus, for the same rating of the converter, the closer the power factor gets to unity, the more active power can be delivered [10, 11].

Operational advantages of a SG with power electronics converters are numerous, like for example voltage regulation which is handled by the grid-side-converter. Another advantage is that dynamic disturbances of the grid and the wind turbine are isolated from each other and SG is not at risk of losing synchronism. Furthermore, starting and synchronising equipment is not needed as this is taken care of by power electronics converter. The only advantage of induction generators (IGs) over SGs is that the converter is not dimensioned for full power. However, with recent decrease in cost of power electronic components, this is not of concern anymore.

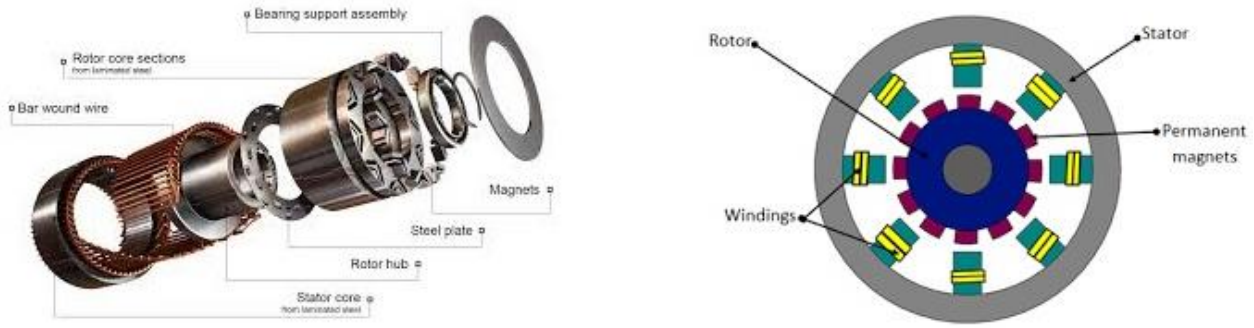

FIGURE I.9 Permanent Magnet Synchronous Generator.

A direct drive tidal energy systems cannot employ a conventional high speed (and low torque) electrical machines. In [10] has shown that the weight and size of electrical machines increases when the torque rating increases for the same active power. Therefore, it is essential task of the machine designer to consider an electrical machine with high torque density, in order to minimise the weight and the size. It has also been shown that PM synchronous machines have higher torque density compared with induction and switched reluctance machines. Thus a PMSG is chosen for further studies in this work. However, since the cost effectiveness of PMSG is an important issue, low manufacturing cost has to be considered as a design criterion in further steps. There are a number of different PMSG topologies, some of them are very attractive from the technical point of view. However, some of the state of the art topologies suffer from complication in manufacturing process which results in high production costs. PM excitation offers many different solutions. The shape, the size, the position, and the orientation of the magnetisation direction can be arranged in many different ways [10, 12].

6.1 Permanent-Magnet Synchronous Generator dq-Model

The permanent magnet synchronous generator (PMSG) uses buried rare earth magnets. Its electrical behaviour is described by the well known dq model, given by

$$v_{dq} = R_{dq} i_{dq} + L_{dq} \frac{di_{dq}}{dt} + p\omega_m \Im(L_{dq} i_{dq} + \psi_f) \quad \text{(I. 7)}$$

Where, $\psi_f = \begin{bmatrix} \phi_f \\ 0 \end{bmatrix}$ represents the vector of the flux linkages, $i_{dq} = \begin{bmatrix} i_d \\ i_q \end{bmatrix}$ represents the vector of the stator currents, $R_{dq} = \begin{bmatrix} R_S & 0 \\ 0 & R_s \end{bmatrix}$ represents the matrix of the stator resistance, $\Im = \begin{bmatrix} 0 & -1 \\ 1 & 0 \end{bmatrix}$, $v_{dq} = \begin{bmatrix} v_d \\ v_q \end{bmatrix}$ represents the vector of the voltage stator, and $L_{dq} = \begin{bmatrix} L_d & 0 \\ 0 & L_q \end{bmatrix}$ represents the matrix of the stator inductions.

The mechanical equation of the PMSG is given by

$$J \frac{d\omega_m}{dt} + f_{fv} \omega_m = T_m - T_{em} \quad \text{(I. 8)}$$

Where, T_e is the electromagnetic torque, J represents the total inertia of the system, and f_{fv} is the viscous coefficient. The electromagnetic torque T_{em} can be expressed in the dq frame as follows

$$T_e = \frac{3}{2} p\big(L_d - L_q\big) i_d i_q + \phi_f i_q \quad \text{(I. 9)}$$

The interdependence between the induced flux linkage in the PMSG ψ_{dq} and the currents vector i_{dq} is given by

$$\psi_{dq} = \begin{bmatrix} \psi_d \\ \psi_q \end{bmatrix} = \begin{bmatrix} L_d i_d + \phi_f \\ L_q i_q \end{bmatrix} \quad \text{(I. 10)}$$

Where ψ_d and ψ_q are the flux linkages in the dq frame, and ϕ_f represents the flux linkages due to the permanent magnets.

Substituting the i_{dq} value obtained from (10) in Eqs. (7) and (9) yields

$$\frac{d\psi_{dq}}{dt} - p\omega_m \Im \psi_{dq} = v_{dq} - R_{dq} i_{dq} \quad \text{(I. 11)}$$

6.2 Permanent-Magnet Synchronous Generator αβ-Model

The PMSM uses rare earth surface mounted magnets with no significant aliency effects. The standard two phases αβ- model of PMSG obtained via direct application of EL equations is given by

$$L_{\alpha\beta}\frac{di_{\alpha\beta}}{dt} + \psi_{\alpha\beta}(\theta_e)p\omega_m = v_{\alpha\beta} - R_{\alpha\beta}i_{\alpha\beta} \quad (\text{I. 12})$$

$$J\frac{d\omega_m}{dt} = T_m - T_e\left(i_{\alpha\beta}, \theta_e\right) - f_{fv}\omega_m \quad (\text{I. 13})$$

$$T_e\left(i_{\alpha\beta}, \theta_e\right) = \psi_{\alpha\beta}^T(\theta_e)i_{\alpha\beta} \quad (\text{I. 14})$$

Where, T_e denotes the electromagnetic torque in αβ-frame, $\psi_{\alpha\beta}(\theta_e) = \psi_f\begin{bmatrix}-\sin(\theta_e)\\ \cos(\theta_e)\end{bmatrix}$ is the flux linkages vector in αβ-frame, $i_{\alpha\beta} = \begin{bmatrix}i_\alpha\\ i_\beta\end{bmatrix}$ represents the stator current vector in αβ-frame, $L_{\alpha\beta} = \begin{bmatrix}L_\alpha & 0\\ 0 & L_\beta\end{bmatrix}$ denotes the stator induction matrix in αβ-frame, $R_{\alpha\beta} = \begin{bmatrix}R_S & 0\\ 0 & R_s\end{bmatrix}$ represents the stator resistance matrix in αβ-frame, $v_{\alpha\beta} = \begin{bmatrix}v_\alpha\\ v_\beta\end{bmatrix}$ denotes the voltage stator vector in αβ-frame, and $\theta_e = p\omega_m$ represents the electrical angular velocity [10].

7 Control Strategies for PMSG-based Tidal Conversion Systems

In renewable power generation, the tidal energy has been noted as the most swiftly growing technology. It draws interest as one of the most money-spinning ways to generate electricity from renewable sources. Recently, voltage source converter (VSC) based permanent magnet generator (PMSG) tidal turbine is assessed to be higher ranked than doubly fed induction generator (DFIG) tidal turbine in terms of reliability and efficiency. The variable speed tidal turbine with a direct drive multi pole PMSG with fully controllable voltage source converters is catching market progressively specially in offshore applications. Among the various power electronics topologies used in tidal energy conversion system, the most promising one is permanent magnet synchronous generator (PMSG) with a full-scale back-to-back power converter. The basic components in Tidal energy conversion system (TECS) include tidal turbine, an electric generator (PMSG) and power electronic interface. Tidal energy conversion system is interfaced with the utility system through power electronic converters. However, the high performance controller design for PMSM is still a

challenging work, because numerous issues still need to be addressed, such as varying operating conditions, parametric uncertainties, unknown modeling errors, unstructured system dynamics and external disturbances.

During the past decades, extensive control theories and techniques have been proposed for PMSM, including classical and robust control laws. In [13], a new control for a PMSG-based tidal conversion system is proposed, namely a second-order active disturbance rejection control (ADRC) approach which is applied to fully maintain the advantages of "large error, small gain; small error, large gain" compared to classical ADRC. Figure I.10 shows a classical double-loop control scheme of a permanent magnet synchronous generator (PMSG), the current loop control is usually based on PI controllers, and the speed controller can be either PI controller or another advanced controller.

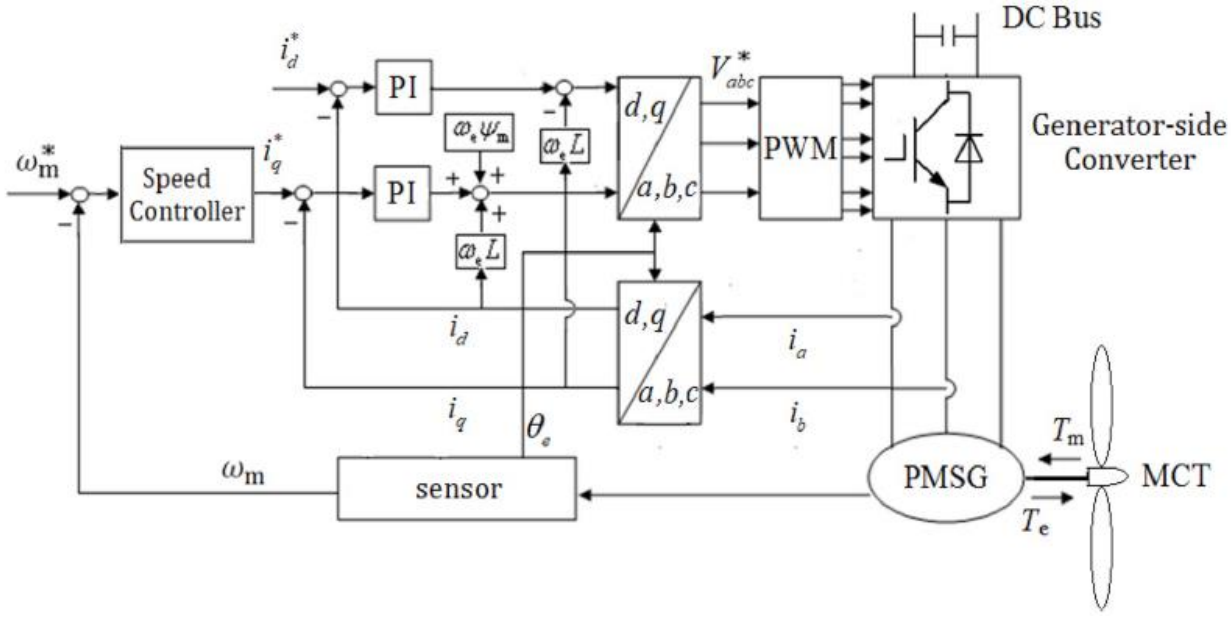

FIGURE I.10 Conventional PI controller of the PMSG.

In order to fully benefit from the ADRC strategies advantages, an all-ADRC approach, as shown in Figure I.11, is proposed in this work. In this approach, all the controllers both in speed and current loops are designed by ADRC strategies. In the proposed cascaded ADRC approach, the decoupling terms in the classical PI current control loops are not needed and thus the dependence of system parameters can be reduced. Using a higher order ADRC controller to combine the speed ADRC controller and the *q*-axis ADRC current controller can achieve a possible variant of this ADRC approach.

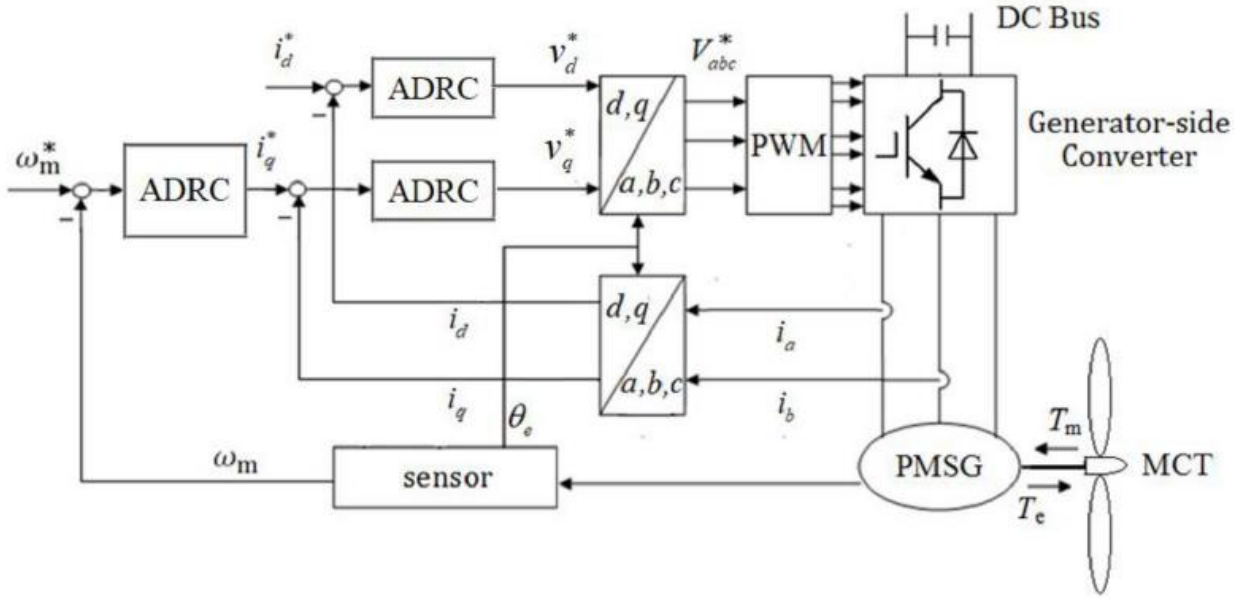

FIGURE I.11 Second-order cascaded ADRC of the PMSG.

A resilient control of a permanent magnet synchronous generator-based tidal turbine subjected to magnet failures is proposed in [14]. In this context, a magnetic equivalent circuit method is used to model the synchronous generator magnet failures. A fault-resilient controller is therefore derived for magnet failure resilience purposes (Figure I.12). In fact, high-order sliding modes have been adopted to address the robustness problems faced by conventional techniques such as PI controller (see Figure I.10).

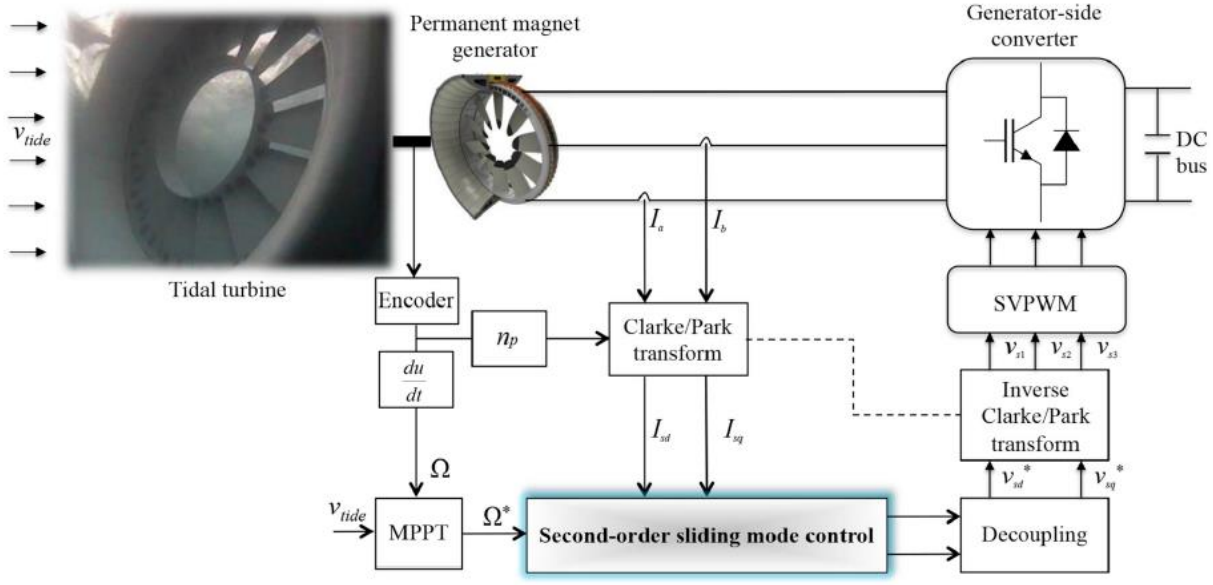

FIGURE I.12 Fault-resilient controller ADRC of the PMSG.

High-order sliding modes, namely the second-order ones, are adopted for resilient-control of the permanent magnet synchronous generator-based tidal turbine experiencing demagnetization. Indeed, such kind of robust control approach has been extensively used for wind and tidal systems, where it has been demonstrated their ability to achieve simple control algorithms and chattering-free phenomenon in a finite-time.

A new fuzzy terminal sliding mode control strategy is proposed to extract the maximum marine current energy. The control strategy as illustrated in Figure I.13, mainly consists of a fuzzy logic controller for deriving the reference q-axis generator current and a non-singular terminal sliding mode current controller capable of accurately tracking the derived reference generator current. A swell filter is also involved in the control strategy to improve the generator power quality in case of swell effects. The detailed design process and stability condition analysis of this control strategy have been thoroughly investigated [15].

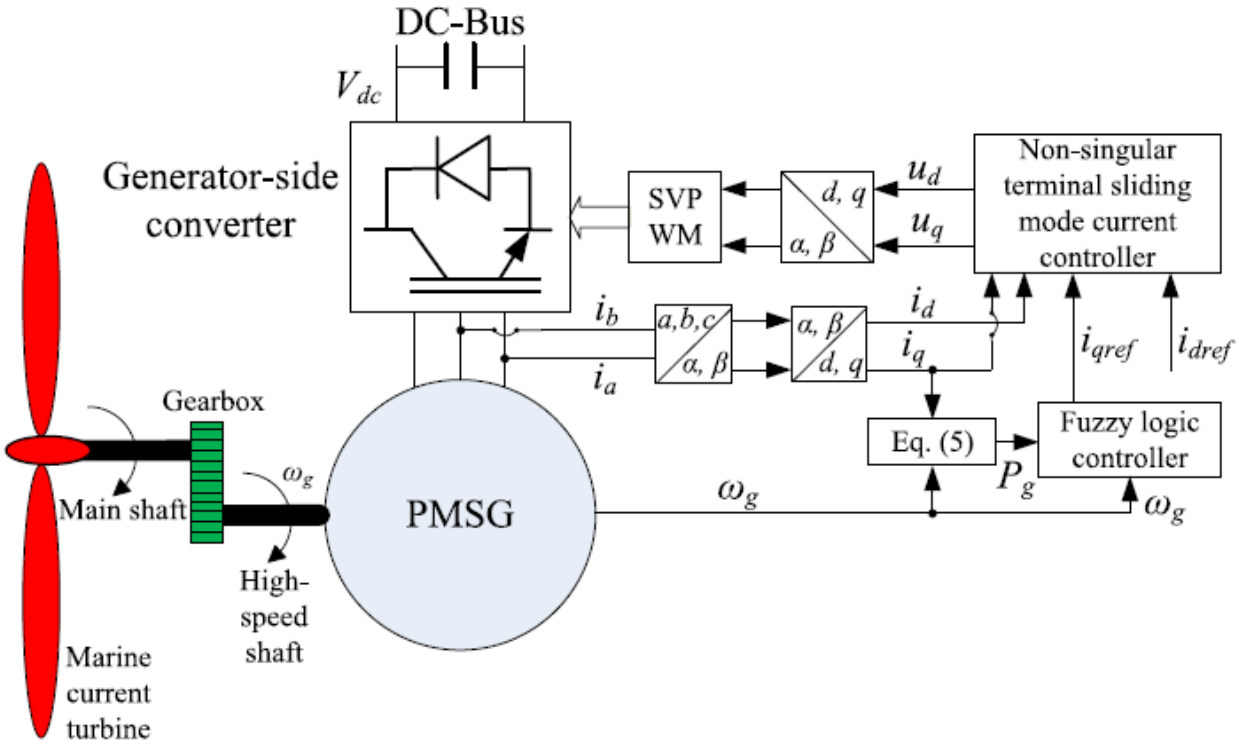

FIGURE I.13 Fuzzy terminal sliding mode control of the PMSG.

Experimental validation of a Matlab-Simulink simulation tool of marine current turbine (MCT) systems is demonstrated in [16]. The developed simulator is intended to be used as a sizing and site evaluation tool for MCT installations. For that purpose, the simulator is evaluated within the context of speed control of a permanent magnet synchronous generator based (PMSG) MCT. To

increase the generated power, and therefore the efficiency of an MCT, a nonlinear controller has been proposed. PMSG has been already considered for similar applications, particularly wind turbine systems using mainly PI controllers. However, such kinds of controllers do not adequately handle some of tidal resource characteristics such as turbulence and swell effects. Moreover, PMSG parameter variations should be accounted for. Therefore, a robust nonlinear control strategy, namely second-order sliding mode control, is proposed. The proposed control strategy is inserted in the simulator that accounts for the resource and the marine turbine models. Simulations using tidal current data from Raz de Sein (Brittany, France) and experiments on a 7.5-kW real-time simulator are carried out for the validation of the simulator (see Figure I.14).

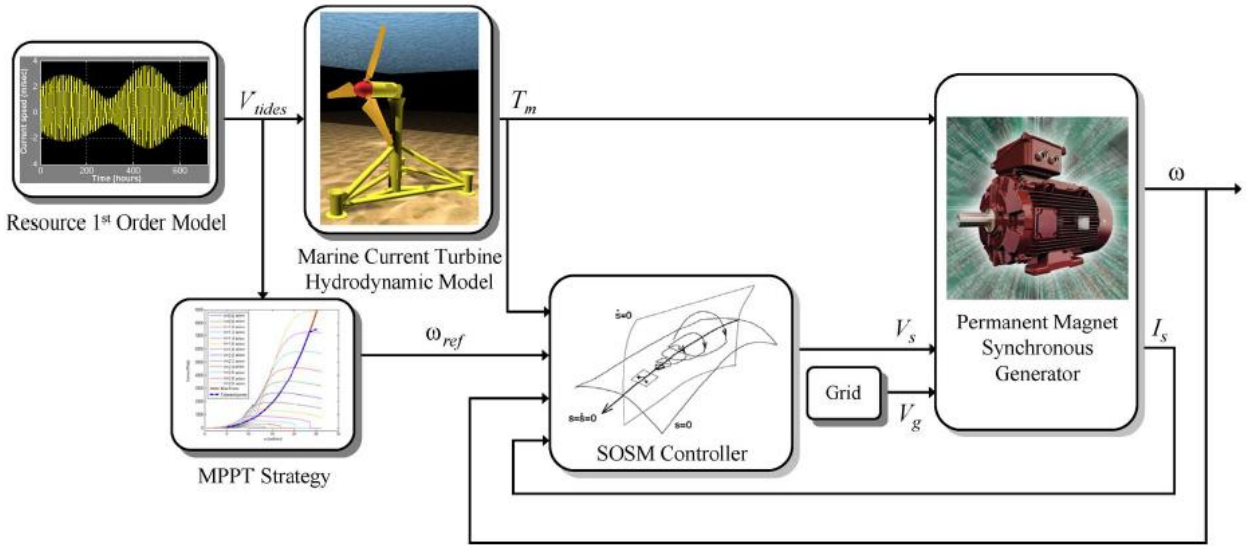

FIGURE I.14 Sliding mode control of the PMSG.

Flux-weakening strategy is investigated in [17] to realize appropriate power control strategies at high marine current speeds. During flux-weakening operations, the generator can be controlled to produce nominal or overnominal power for a specific speed range (constant power range). These two power control modes are compared, and the constant power range is calculated. The relationship between the expected constant power range and generator parameter requirements [stator inductance, permanent magnet (PM) flux, and nominal power coefficient] is analyzed. A Torque-based control with a robust feedback flux-weakening strategy is then carried out in the simulation. The proposed control strategies are tested in both high tidal speed and swell wave cases. The achieved simulation results have confirmed that, at overrated current speed, the constant active power mode enables to limit the generator output power to the nominal value with lower losses,

while the maximum active power mode enables to produce over-nominal power (better use the generator-side converter– rating) but with high copper losses. The parameter requirements of the nonsalient PM machine for expected constant power speed ratio are provided in this paper. The compromise between high power factor and large constant power range should be noted for

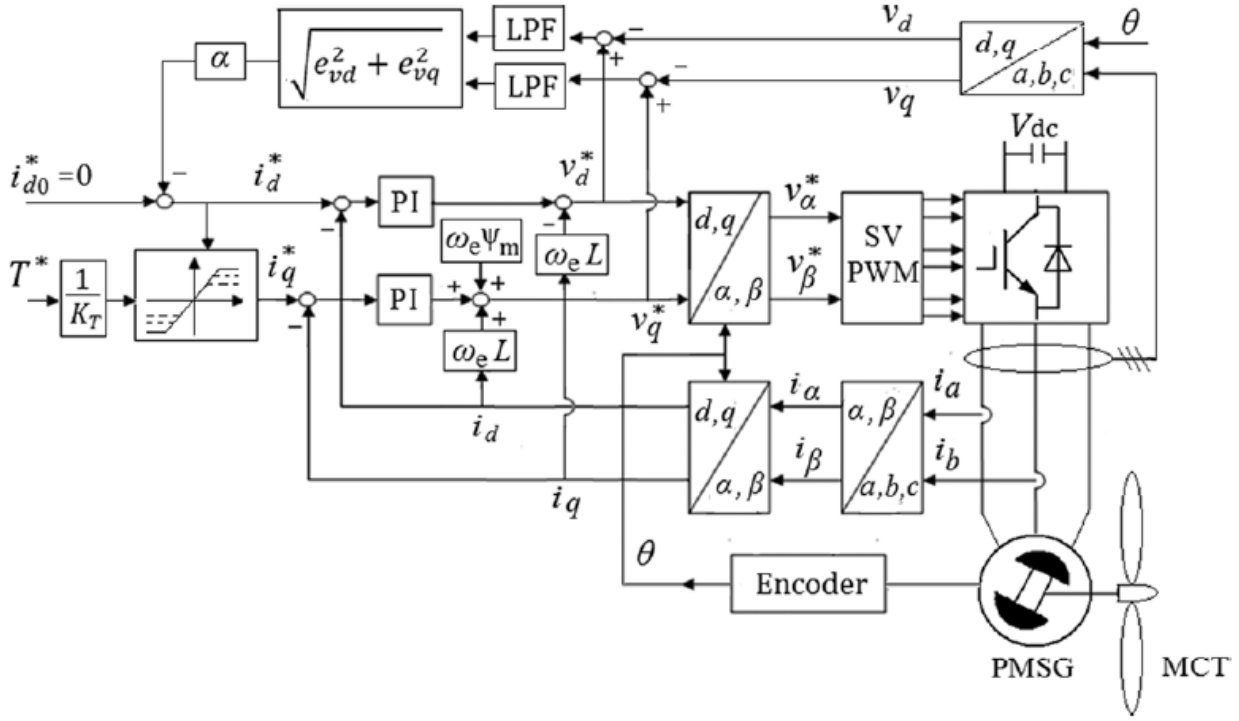

FIGURE I.15 Flux-weakening strategy of the PMSG.

An adaptive Takagi–Sugeno (T–S) fuzzy model predictive control (ATSFMPC) scheme is proposed for the design of a PMSG-HTs as illustrated in Figure I.16. The main objective is to maintain the maximum hydrokinetic energy extraction, i.e., tracking a specified rotational speed of the PMSG when random fluctuations due to the uncertainty of tidal flow are incorporated. To derive the reference torque and stator flux of the PMSG at the maximum power point, an ocean current meter is employed to measure the ocean flow speed before the maximum power point tracking (MPPT) scheme is used to estimate the reference angular speed of the generator. Next, using the maximum torque per ampere control (MTPA) approach, the reference torque and stator flux of the PMSG could be extracted as the tracking target for the model predictive torque control (MPTC) strategy. In addition, to represent the PMSG–based nonlinear hydrokinetic turbine systems, the adaptive T–S fuzzy model is presented to establish the approximate model. The designed scheme is capable of concurrent estimations of the stator current and voltage along the d–

axis and the q-axis. Finally, a model predictive torque controller for the PMSG system is employed to indirectly control the stator current and the stator flux magnitude, which improves the control performance and achieves maximum hydropower tracking [18].

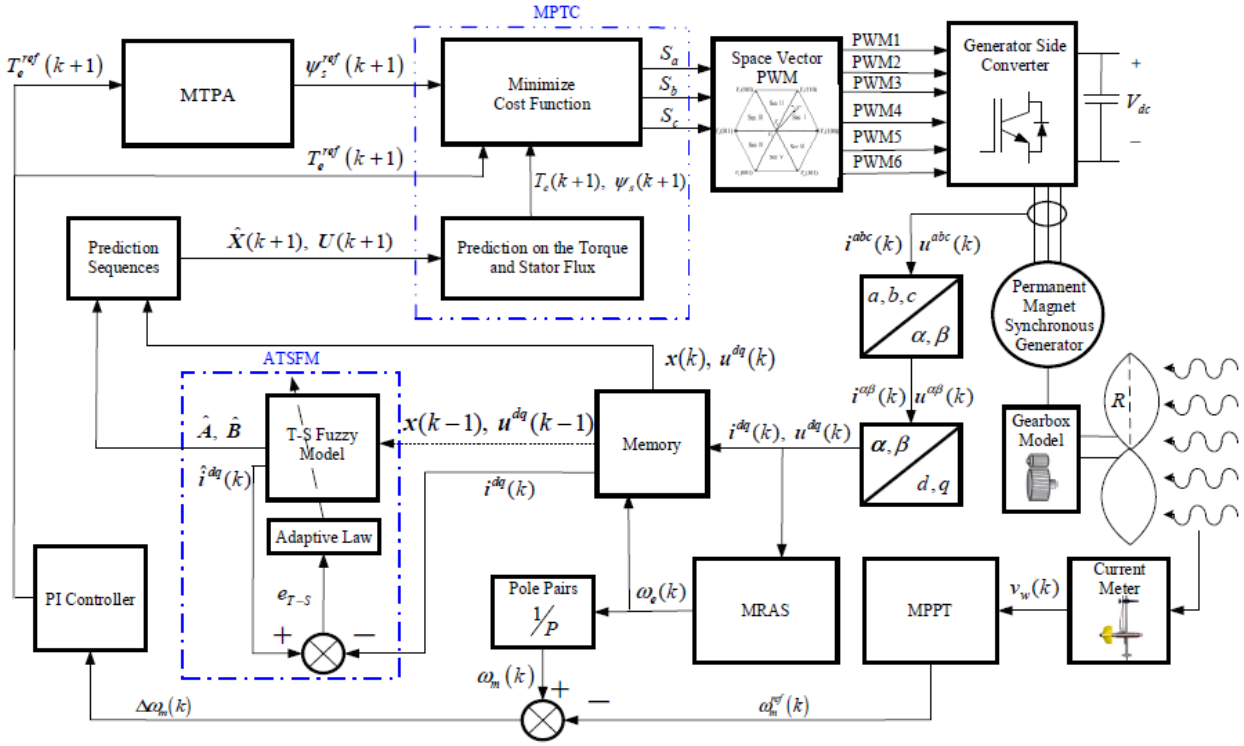

FIGURE I.16 Adaptive Takagi–Sugeno (T–S) fuzzy model predictive control of the PMSG.

8 The problematic of this thesis

In this thesis, the control problem is challenging for at least two reasons. First, how to control the PMSG so that it generates the power received at its input, as the dynamics of the conversion system are described by a highly coupled set of nonlinear differential equations and various uncertainties of the PMSG model. Second, it is preferable to operate this kind of systems at the point of maximum power, which is a nonlinear function. Thus, the design of a controller that take in consideration the major part of these issues is the principal aim of the present work.

9 Conclusion

This chapter has introduced up-to-date in large marine current turbine technologies and reviewed state of the art of tidal energy technologies. The emphasis has been put on challenges of power extraction from tidal current turbine systems. The characteristics and the strength/weakness of various energy storage system technologies have been presented for tidal energy application. It has been shown that PMSG-based tidal turbine conversion system connected to the grid is the most

investigated in the literature and industry. A comparison between the PMSG and the DFIG has been performed for the application in tidal current conversion. it has also shown that the use of the PMSG in this kind of underwater applications, presents numerous inconvenient and an adequate controller is needed to improve its performances. A state of art of the nonlinear controls proposed in the literature concerning the PSMG has also reviewed.

References

[1] Zhou, Z., Benbouzid, M. E. H., Charpentier, J. F., Scuiller, F., Tang, T. Developments in large marine current turbine technologies - A Review. Renewable and Sustainable Energy Reviews, 2017; 71: 852-858.

[2] Hafeez N, Badshah S, Badshah M, Khalil SJ. Effect of velocity shear on the performance and structural response of a small-scale horizontal axis tidal turbine. Marine Systems & Ocean Technology, 2019; 14(2): 51-58.

[3] Othman AM. Enhancement of tidal generators by superconducting energy storage and jaya-based sliding-mode controller. International Journal of Energy Research, 2020; 44(14): 11658-11675.

[4] Benzerdjeb A, Abed B, Achache H, Hamidou MK, Gorlov AM. Experimental study on blade pitch angle effect on the performance of a three-bladed vertical-axis Darrieus hydro turbine. Int. J. Energy Res., 2019; 43: 2123-2134.

[5] Saini G, Saini RP. A review on technology, configurations, and performance of cross-flow hydrokinetic turbines. Int. J. Energy Res., 2019; 43: 6639-6679.

[6] Bajaj M, Singh AK. Grid integrated renewable DG systems: A review of power quality challenges and state-of-the-art mitigation techniques. Int. J. Energy Res., 2020; 44: 26-69.

[7] Zhang Y, Rodriguz EF, Zheng J, Zheng Y, Zhang J, Gu H, Zang W, Lin W. A review on numerical development of tidal stream turbine performance and wake prediction. IEEE Access, 2020; 8: 79325-79337.

[8] Qian P, Feng B, Liu H, Tian X, Si Y, Zhang D. Review on configuration and control methods of tidal current turbines. Renewable and Sustainable Energy Reviews, 2019; 108: 125-139.

[9] E. Muljadi, Y. H. Yu, “Review of marine hydrokinetic power generation and power plant,” Electric Power Components and Systems, vol. 43, no. 12, pp. 1422-1433, 2015.

[10] Achour AY. Passivity based control of Electromechanical systems. Thesis on French, PhD dissertation, Bejaia University, Algeria, Oct. 2009.

[11] Pérez GE, Alcantar MG, Ramérez GG. Passivity-based control of synchronous generators. Proceeding of the IEEE International Symposium on Industrial Electronics (ISIE '97), 1997; 1: 101-106.

[12] Guzman VMH, Ortigoza RS, Sakanassi JAO. Energy-based control of electromechanical systems. Advances in Industrial Control, Springer, 2021.

[13] Zhou Z, Elghali BS, Benbouzid MEH, Amirat Y, Elbouchikhi E, Feld G. Tidal stream turbine control: An active disturbance rejection control approach. Ocean Engineering, 2020; 202: 107190.

[14] Toumi S, Elbouchikhi E, Amirat Y, Benbouzid M, Feld G. Magnet failure-resilient control of a direct-drive tidal turbine. Ocean Engineering, 2019; 187: 106207.

[15] Gu Y-j, Yin X-x, Liu H-w, Li W, Lin Y-g. Fuzzy terminal sliding mode control for extracting maximum marine current energy. Energy, 2015; 90(1): 258-265.

[16] Benelghali, S., Benbouzid, M. E. H., Charpentier, J. F., et al. Experimental validation of a marine current turbine simulator: application to a permanent magnet synchronous generator-based system second-order sliding mode control. IEEE Trans. Ind. Electron, 2011; 58(1): 118-126.

[17] Zhou, Z., Scuiller, F., Charpentier, J. F., Benbouzid, M. E. H., Tang, T. Power smoothing control in a grid-connected marine current turbine system for compensating swell effect. IEEE Transaction on Sustainable Energy, 2013; 4(3): 816-826.

[18] Yin, X., Zhao, X. Sensorless maximum power extraction control of a hydrostatic tidal turbine based on adaptive extreme learning machine. IEEE Transaction on Sustainable Energy, 2020; 11(1): 426-435.

Chapter II

Passivity-Based Control: A Review

1 Introduction

Passivity is a fundamental property of many physical systems which may be roughly defined in terms of energy dissipation and transformation. It is an inherent Input-Output property in the sense that it quantifies and qualifies the energy balance of a system when stimulated by external inputs to generate some output. Passivity is therefore related to the property of stability in an input-output sense, that is, we say that the system is stable if bounded "input energy" supplied to the system, yields bounded output energy. This is in contrast to Lyapunov stability which concerns the internal stability of a system, that is, how "far" the state of a system is from a desired value. Passivity is a concept that is closely related to electric circuits and mechanical systems and, thus, passivity is well suited for the study of electromechanical systems. In electric circuits, for instance, the basic phenomena are described by inductances, capacitances, and resistances. These circuit elements have the property to either store energy (inductors and capacitors) or dissipate energy (resistors). Moreover, energy stored by inductors and capacitors is never greater than energy that they receive and energy dissipated by resistors is never greater than energy that they receive. This means that inductances, capacitances, and resistances do not generate energy and, because of that, they are called passive circuit elements. In other words, how differently a system behaves with respect to a desired performance. Passivity based control is a methodology which consists in controlling a system with the aim at making the closed loop system, passive [1,2].

The field constitutes an active research direction and therefore in this chapter we give only a basic overlook of the most important concepts involved. A section is also devoted to a wide class of physical passive systems: the Euler-Lagrange (EL) systems and their passivity-based control. The reader should rather consider this presentation as very concise image of the material cited in the Bibliography. Therefore, we invite the reader who wishes to obtain a deeper knowledge in the subject, to see those references [3,4].

2 Passivity Based Control

To better understand the passivity concept and passivity-based control (PBC), we need to leave behind the notion of state of a system and think of the latter as a device which interacts with its environment by transforming inputs into outputs. From an energetic viewpoint we can define a passive system as a system which cannot store more energy than is supplied by some "source",

with the difference between stored energy and supplied energy, being the dissipated energy. Hence, it shall be clear that passivity is closely related to the stability of a system, in the input-output sense evoked in the Summary. In PBC achieving stability from this viewpoint is the first goal. A fundamental property of passive systems is that, regarding a feedback interconnection of (other physical) passive systems, passivity is invariant under negative feedback interconnection. In other words, the feedback interconnection of two passive systems yields a passive system. Thus, if the overall energy balance is positive, in the sense that the energy generated by one subsystem, is dissipated by the other one, the closed loop will be stable in an input-output sense. This property constitutes the basis of passivity-based control (PBC) (see Figure II.1) [4,5].

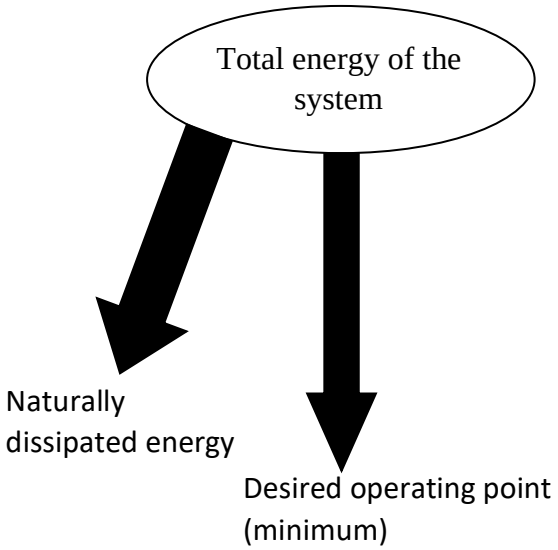

FIGURE II.1 Naturally dissipation of the system energy.

To that end, we must keep in mind that passivity is a property of the system, seen as an operator which maps inputs into outputs. In this respect, we will find characterizations and sufficient conditions for passivity, which apply to systems that can be modeled by rational transfer functions as well as to systems modeled by nonlinear (possible time-varying) differential equations. We consider a dynamical nonlinear system expressed such that [6]:

$$\begin{cases} \dot{x} = f(x,u) \\ y = h(x,u) \end{cases} \tag{II.1}$$

Where, $\dot{x} \in R^n$ denotes the state, $u \in R^p$ and $y \in R^p$ are the input and the output, respectively with $f(0) = 0$, $h(0) = 0$.

Definition 1. The system (9) is said to be passive if there exists a non-negative function $V(x)$ called the storage function such that:

$$V(x)-V(x_0)\le\int_0^t y^T(\tau)u(\tau)d\tau \tag{II.2}$$

Where, $x(0)=x_0\in R^n$.

If, in addition there is a positive definite function $S:R^n\to R$ such for all $u\in R^p$ and all $x_0\in R^n$:

$$V(x)-V(x_0)\le\int_0^t y^T(\tau)u(\tau)d\tau-\int_0^t S(x(\tau))d\tau \tag{II.3}$$

Then the system (9) is said to be strictly passive.

3 Passivity Based Control: Stat of The Art

The term PBC was first introduced in [7] to define a controller methodology whose aim is to render the closed-Ioop passive. This objective seemed very natural within the context of adaptive control of robot manipulators, since as shown in that paper the robot dynamics defines a passive map, and it had been known since the early work of Koditschek [8] that parameter estimators are also passive. The PBC approach presented in this thesis may be viewed as an extension of the by now well-known energy-shaping plus damping injection technique introduced to solve state-feedback set point regulation problems in fully actuated robotic systems by Takegaki and Arimoto in [9]. This methodology has been instrumental in the solution of several robotics problems [10,11], which were untractable with other stabilization techniques. Passivity concept has gained importance in many control areas. Passivity was used originally in classical mechanics problems and then it was extended to control problems [12]. Passivity-based control with energy molding for induction motors was carried out in [13]. The passivity-based control for PMSM was carried out by Qiu [14]. Achour et al [15] developed a passivity-based current control. The authors proposed to use the magnetic fluxes as the state variables instead of the currents for a PMSM. The PBC can also be found in other engineering applications such as in the smart grid [16], Building [17], recent advances of passivity theory in Cyber-physical systems in [18], Electric vehicle [19], Food systems [20].

Power systems play an important role in the currmt development of every society since the nurriber of tasks that require decrtrica1 energy is increasing day by day. From a control point of view these systems impose a very interesting problme since their dynamic behaviour is described by a mathematical nonlinear model [21]**.** One of the basic elements of this kind of systems are synchronos gencrators, which are intended for transforming into electrical energy the mechanical energy delivered by some source, usually turbines. In this sense, the control of these machines becomes in a problem that must be considcred at a fiindaniental level.

The PBC was introduced to control general rotating electrical machine by [22] and instrumented as a solution for a synchronous generator [23]. Several publications including some variants of this approach applied to the PMSG have been appeared in literature. A standard nonlinear passivity-based control that ensures asymptotic convergence to the maximum power point of wind system connected to a battery, and rendered adaptive is proposed [24], where the adaptation mainly consist on the wind speed estimated, the standard PBC is a variation of PBC that is principally used for systems described by Euler-Lagrange equations [25]. The similar work was considered in [26], replacing the battery by the DC-link with grid-connection, this modification has significantly complicated the control problem. So, a PI-PBC is proposed to control the grid-side to compensate the coupling term from the PMSG-based wind turbine. In [27], the interconnection and damping assignment passivity-based control (IDA-PBC) approach is investigated. Contrary to the classical PBC, the IDA-PBC doesn't propose the storage function of the closed-loop, but it derives as a result of the choice of the interconnection and damping structures of the system. A passivity-based sliding mode control to achieve MPPT of the PMSG-based system is presented in [28], where the aim is to enhance the system robustness by incorporate a sliding-mode control (SMC) to the PBC. The authors in [29], presented on the same conversion model a passivity-based linear feedback control for PMSG which attempts to achieve MPPT, where the sliding-mode control is replaced by a linear feedback control. A passivity-based voltage control is also developed by *Belkhier et al* in [30], to improve the performance of the PMSG dedicated to the tidal current conversion system, which is the first application of the PBC in this area. [31], investigated a passivity-based control associated with two other methods, the fuzzy logic control and the integral sliding-mode control for the PMSG to gain the asymptotically stability by constructing a suitable fuzzy Lyapunov function. An intelligent PBC combined with adaptive backstepping control was investigated by *Belkhier et al*., in [32] to get an optimal extraction of the marine current power by the PMSG.

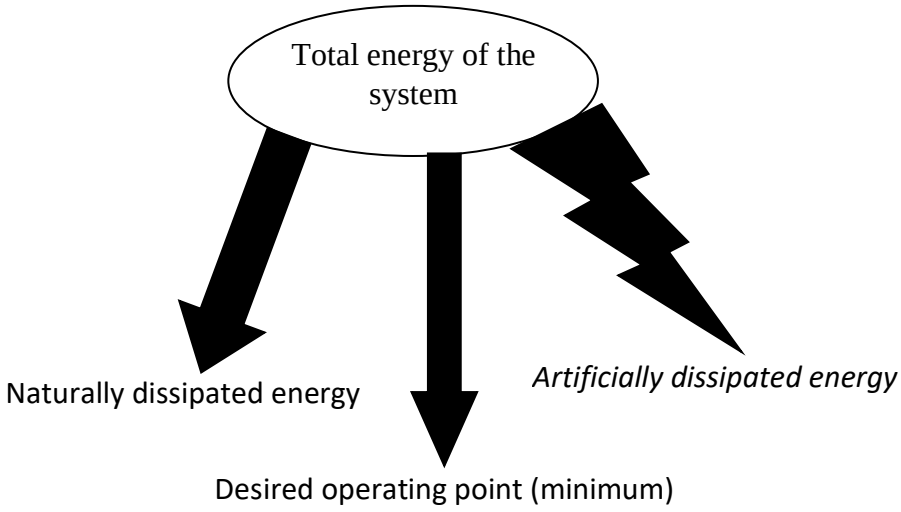

FIGURE II.2 System energy modification and damping injection.

The design of the PBC is reduced to the following three steps [4]:

First Step:

- Representation of the system in energetic form, using EL equations.
- Check the passivity of the controlled system in open-loop.
- Decomposition of the system into two sub-systems interconnected by negative feedback.
- Check the passivity of each sub-systems

Second Step:

- Modification of the model of the system using the vector of non-dissipating forces based on controller system passivity in open-loop (see Figure II.2).
- Establishment of the desired dynamics using the modified model of the system illustrated by Figure II.3.

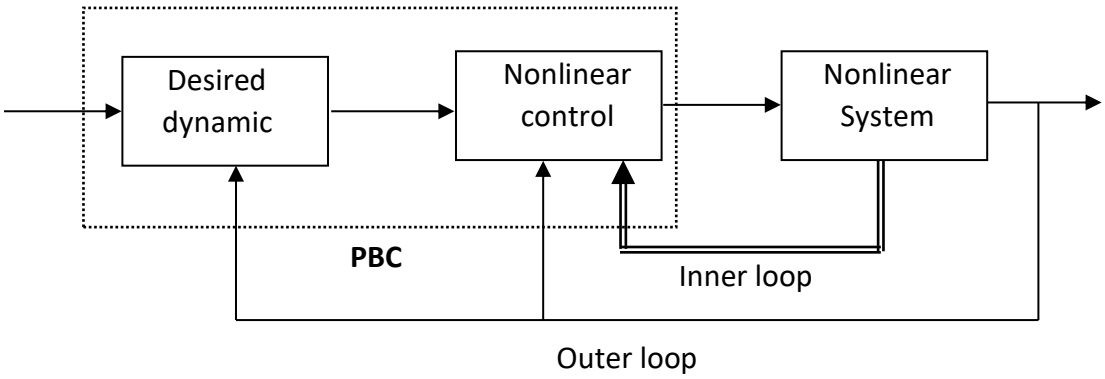

FIGURE II.3 Passivity principe diagram.

Third Step:

- Calculation of the desired coordinates using the desired dynamics.
- Calculation of the error dynamics (between measured and desired coordinates).
- Invocation of stability in the sense of Lyapunov, controller design and a damping term is injected to make the system passive (see Figure II.2).
- Check the passivity of the controlled system in closed-loop.

4 Conclusion

In this chapter, a review on the passivity-based control and the up-to-date has been introduced. The it has been shown that the passivity theory is investigated largely in the literature and industry. Also, a state of the art of the PBC applied to the PMSM has been reported. It has been depicted also, that the PBC was more applied to the PMSG especially in renewable energies. The aforementioned theory has been adopted in the rest of this thesis and investigated on the PMSG-based tidal turbine.

References

[1] Guzman VMH, Ortigoza RS, Sakanassi JAO. Energy-based control of electromechanical systems. Advances in Industrial Control, Springer, 2021.

[2] Ortega R, Jiang ZP, Hill DJ. Passivity-based control of systems: A Tutorial. Proceedings of the American Control Conference, Albuquerque, New Mexico, 1997 : 2633-2637.

[3] Ortega R, Borja P. Passivity-based control. Encyclopedia of Systems and Control: Springer, 2020. https://doi.org/10.1007/978-1-4471-5102-9 100072-1.

[4] Achour AY. Passivity based control of Electromechanical systems. Thesis on French, PhD dissertation, Bejaia University, Algeria, Oct. 2009.

[5] Achour AY. Passivity Based Control for a Permanent Magnet Synchronous Motors, Recent Advances in Robust Control Theory Application in Robotics and Electromechanics" Edt Intech-Open Acess Publisher, Book chapter, 2011: 371-396.

[6] Petrovic V, Ortega R, Stankovic. Interconnection and Damping Assignment Approach to Control of PM synchronous motors. IEEE Trans., Cont. Syst. Tech., 2001; 9(6): 811-820.

[7] Arnold VI. Mathematical method of classical mechanichs. Eds. New York: Springer, 1989.

[8] Koditschek DE. Natural motion of robot arms. In Proc. 23rd. IEEE Conf. Decision Contr., Las Vegas, NV., 1984. [Passivity based control of EL systems and in particular mechanical systems.]

[9] M. Takegaki and S. Arimoto, "A new feedback for dynamic control of manipulators," ASME J. Dyn. Syst. Meas. Contr., 1981: 119-125.

[10] Ren C, Ding Y, Ma S, Hu L, Zhu X. Passivity-based tracking control of an omnidirectional mobile robot using only one geometrical parameter. Control Engineering Practice, 2019; 90: 160-168.

[11] H. Berghuis et H. Nijmeijer: "A passivity Approach to Controller-Observer Design for Robots", IEEE Transaction on Robotics and Automation, 1993; 9(6): 740-754.

[12] Achour AY, Mendil B. Passivity based voltage controller-observer design with unknown load disturbance for permanent magnet synchronous motor. IEEE 23rd International Symposium on Industrial Electronics (ISIE), 2014: 201-206.

[13] Ortega R, Espinoza-Pérez G. Passivity-based control with simultaneous energy-shaping and damping injection: The induction motor case study. In: Proceedings of 16th IFAC world congress. Proceeding in CD, Track.We-E20-TO/3. 2005.

[14] Qiu J, Zhao G. PMSM control with port-controlled Hamiltonian theory. In: Proceedings of 1st international conference on innovative computing, information and control. vol. 3. 2006.

[15] Achour AY, Mendil B, Bacha S, Munteanu I. Passivity-based current controller design for a permanent-magnet synchronous motor. ISA Transactions, 2009; 48(3): 336-346.

[16] Gu Y, Li W, He X. Passivity-based control of DC microgrid for self-disciplined stabilization. IEEE Transactions on power systems, 2015; 30(5): 2623 – 2632.

[17] Cornejo C, Icaza LA. Passivity based control of a seismically excited building. 16th Triennial World Congress, Prague, Czech Republic, IFAC, 2005.

[18] Zakeri H, Antsakli PJ. Recent advances in analysis and design of cyber-physical systems using passivity indices. Proc. Of IEEE 27th Mediterranean Conference on Control and Automation (MED), 2019: 31 – 36.

[19] Benmouna A, Becherif M, Depemet D, Ebrahim MA. Novel Energy Management Technique for Hybrid Electric Vehicle via Interconnection and Damping Assignment Passivity Based Control. Renewable Energy, 2019; 17(4): 976 – 985.

[20] Riverol C. Passivity-based control of non-isothermal tank used in the production of pineapple syrup. Food Control, 2001; 12: 373-378.

[21] Abdelrahem M, Hackl CM, Zhang Z, Kannel R. Robust Predictive Control for Direct Driven Surface-Mounted Permanent-Magnet Synchronous Generators Without Mechanical Sensors. IEEE Trans. on Energy Conversion, 2018; 33(1): 179-189.

[22] Nicklasson PJ, Ortega R, Pérez GE. Passivity-based control of the general rotating electrical machine. Proceeding of the 33rd Conference on Decision and Control. Lake Buena Vista, FL, 1994: 4018-4023.

[23] Pérez GE, Alcantar MG, Ramérez GG. Passivity-based control of synchronous generators. Proceeding of the IEEE International Symposium on Industrial Electronics (ISIE '97), 1997; 1: 101-106.

[24] David FM, Ortega R. Adaptive passivity-based control for maximum power extraction of stand-alone windmill systems. Control Engineering Practice, 2012; 20: 173-181.

[25] Ortega R, Spong M. Adaptive motion control of rigid robots: A tutorial. Automatica, 1989; 25: 877-888.

[26] Cisneros R, David FM, Ortega R. Passivity-based control of a grid-connected small-scale windmill with limited control authority. IEEE Journal of Emerging and Selected Topics in Power Electronics, 2013; 1(4): 247-259.

[27] Santos GV, Cupertino AF, Mendes VF, Junior SIS. Interconnection and damping assignment passivity-based control of a PMSG based wind turbine. 2015 IEEE 13th Brazilian Power Electronics Conference and 1st Southern Power Electronics Conference (COBEP/SPEC), Fortaleza, Brazil, 2015.

[28] Yang, B., Yu, H., Zhang, Y., Chen, J., Sang, Y., Jing, L. Passivity-based sliding-mode control design for optimal power extraction of a PMSG based variable speed wind turbine. Renewable Energy, 2018; 119: 577-589.

[29] Yang, B., Yu, T., Shu, H., Qiu, D., Zhang, Y., Cao, P., Jiang, L. Passivity-based linear feedback control of permanent magnetic synchronous generator-based wind energy conversion system: design and analysis. IET Renewable Power Generation, 2018; 12(9): 981-991.

[30] Belkhier Y, Achour AY. Passivity-based voltage controller for tidal energy conversion system with permanent magnet synchronous generator. International Journal of Control, Automation and Systems, 2020; 19: 1-11.

[31] Subramaniam, R., Joo, Y. H. Passivity-based fuzzy ISMC for wind energy conversion systems with PMSG. IEEE Transactions on Systems, Man, and Cybernetics: Systems, 2019: 1-10.

[32] Belkhier, Y., Achour, A. Y. Fuzzy passivity-based linear feedback current controller approach for PMSG-based tidal turbine. Ocean Engineering, 2020; 218.

Chapter III

Passivity-Based Voltage Control for Tidal Energy Conversion System with Permanent Magnet Synchronous Generator

1 Introduction

The majority of marine current conversion technologies are based PMSG that is for their numerous advantages, such as high-power density, clean energy, low cost, and favorable electricity production. However, the maximum power that can extract the tidal turbine is nonlinear, depending on the load demand. Moreover, due to the PMSG time-varying parameters, nonlinear dynamic and external disturbances, make the control design a real task. Furthermore, reactive power support and DC-link over voltage, are considered as the necessary conditions to connect the tidal conversion system to the grid, as indicated in [1, 2]. During the last decades, extensive control theories and techniques have been reported in the literature proposing solutions to the stated PMSG problems. In [3], a jaya-based sliding mode approach to enhance the performances of a tidal conversion system, the authors proposed an association of the tidal system with superconducting magnetic energy system (SCMES), for which, the jaya-based controller is applied. However, this association improve the costs and maintenances time of the conversion system. In [4], a fuzzy sliding mode controller that adaptively extract the maximum tidal power under swell effects, is developed. However, the PMSG parameter changes and uncertainties have not considered. The authors in [5], proposed a novel active disturbance rejection controller as an alternative to the conventional PI control. This strategy treats the parameter uncertainties or changes as an element to be rejected which can be cancelled during the control design. A magnetic equivalent circuit method-based second-order sliding mode is proposed in [6] for a tidal turbine-based PMSG subjected to magnet failures to address robustness problems. However, external disturbances and parameter changes have not been considered.

In the same context, in the present chapter, is proposed a novel passivity-based voltage control (PBVC), that forces the PMSG to track the tidal turbine time-varying speed, and maintain this one operating at the optimal torque. Inherent advantages of the passivity-based control (PBC) strategy are the guaranteed stability, the compensation of the nonlinear terms not by cancellation but in a damped way, and enhanced robustness properties. The system dynamic is decomposed into feedback interconnection of two passive subsystems, its electrical and mechanical dynamics. The PBC is applied only to the direct subsystem (electrical dynamics), while the second, e.g., the mechanical dynamics, is treated as a "passive disturbance", unlike the aforementioned nonlinear

controls, which are usually signal-based, and neglecting the PMSG mechanical part as mentioned in [7]. The PBC was introduced in [8] to control general rotating electrical machine and it has been adopted as a solution for a synchronous generator in [9]. Many publications including some variants of this strategy adopted to control the PMSG have been investigated now by researchers. Literature [10], investigated a passivity-based fuzzy integral sliding-mode control for the PMSG by constructing a suitable fuzzy function. In [11], the interconnection and damping assignment passivity-based control (IDA-PBC) approach is applied to a wind turbine associated to a PMSG. In [12], an adaptive passivity-based controller is proposed to achieve the MPPT. The authors in [13], investigated a passivity-based linear feedback control for which attempts to achieve MPPT.

The maximum power extraction from the tidal turbine, with taking into account its entire dynamic when synthesizing the controller, represents the main motivation of the present work. The other aim of the study consists to maintain the DC-link voltage and the generated reactive power at their reference values, despite the disturbances related to the PMSG nonlinear properties and parametric uncertainties, that is to improve the overall performances of the tidal conversion system, a special focus is given to the generator control, as it's the bridge between the tidal turbine and the grid, that is, by using the new proposed control strategy. Furthermore, the robustness against parameter changes has been taken a special attention. To confirm the performance and the feasibility of the proposed method, numerical tests are carried out under MATLAB software for 1.5 MW PMSG-based tidal turbine connected to the grid via a buck-to-buck converter.

2 Design of the PBVC strategy

The application of the PBVC proposed in this work and combined to the nonlinear observer needs number of steps: First, it is necessary to calculate an Euler-Lagrange model, to choose an appropriate input and output vectors such that the relationship between them is passive. Second, the system has to be decomposed into two interconnected subsystems with negative feedback. Finally, the last step consists to identify the non-dissipative terms in the system model. The controller design process is depicted in Figure III.1, in which, two main parts can be distinguished: In the first, the desired dynamic described by the desired current, which is based on the reference electromagnetic torque, computed by the PID controller. The second part computes the control voltage using the desired dynamic and the damping term. The controller objective is to make the

system passive and forces the PMSG to track tidal turbine speed, by reshaping the closed-loop system energy and injecting a damping term.

By using the PMSG αβ-frame model given in equations (I.12)-(I.14) the desired dynamic is formulated as follow:

$$v_{\alpha\beta}^{*} = L_{\alpha\beta}\frac{di_{\alpha\beta}^{*}}{dt} + \psi_{\alpha\beta}(\theta_e)p\omega_m + R_{\alpha\beta}i_{\alpha\beta}^{*} \tag{III.1}$$

$$T_m = J\frac{d\omega_m^{*}}{dt} - T_e^{*}(i_{\alpha\beta}^{*}, \theta_e) - f_{fv}\omega_m^{*} \tag{III.2}$$

Where, T_e^{*} denotes the desired electromagnetic torque, $v_{\alpha\beta}^{*}$, $i_{\alpha\beta}^{*}$, are respectively the desired voltage and current, and ω_m^{*} is the desired rotor speed. Therefore, the aim is to find $v_{\alpha\beta}$ which ensure the convergence of the dynamic, i.g., the error between the desired dynamics and the measured, to zero. Then, the Eqs. (III.1) and (III.2) are reduced to the following expressions:

$$v_{\alpha\beta} - v_{\alpha\beta}^{*} = L_{\alpha\beta}\frac{d\varepsilon_i}{dt} + R_{\alpha\beta}\left(i_{\alpha\beta}^{*} - i_{\alpha\beta}\right) \tag{III.3}$$

$$J\frac{d\omega_m^{*}}{dt} - T_e^{*}\left(i_{\alpha\beta}^{*}, \theta_e\right) - f_{fv}(\omega_m^{*} - \omega_m) = 0 \tag{III.4}$$

The desired energy for the closed loop system $V_f^{*}(\varepsilon_i)$ is put as follows:

$$V_f^{*}(\varepsilon_i) = \frac{1}{2}\varepsilon_i^{T}\left(L_{\alpha\beta}\varepsilon_i\right) \tag{III.5}$$

Where, $\varepsilon_i = \left(i_{\alpha\beta}^{*} - i_{\alpha\beta}\right)$ is the current tracking error. The time derivative of $V_f^{*}(\varepsilon_i)$ along the trajectory (III.3), yields:

$$V_f^{*}(\varepsilon_i) = -\varepsilon_i^{T}\left(R_{\alpha\beta}\varepsilon_i + \left(v_{\alpha\beta} - v_{\alpha\beta}^{*}\right)\right) \tag{III.6}$$

We deduce the following dynamic to ensure the fast convergence to zero of the currents vector error, by tracking the control law:

$$v_{\alpha\beta} = v_{\alpha\beta}^{*} - B_i\varepsilon_i \tag{III.7}$$

Where $B_i = b_i I_2$ is a 2-by-2 matrix of positive gains, and I_2 identity matrix.

Remarque 1. With high gains b_i, the positive definite matrix B_i will address the parameter uncertainties of the system in the closed-loop system, and increases the convergence of the tracking error.

The proof of the fast convergence to the desired state trajectory, is given by Appendix A.

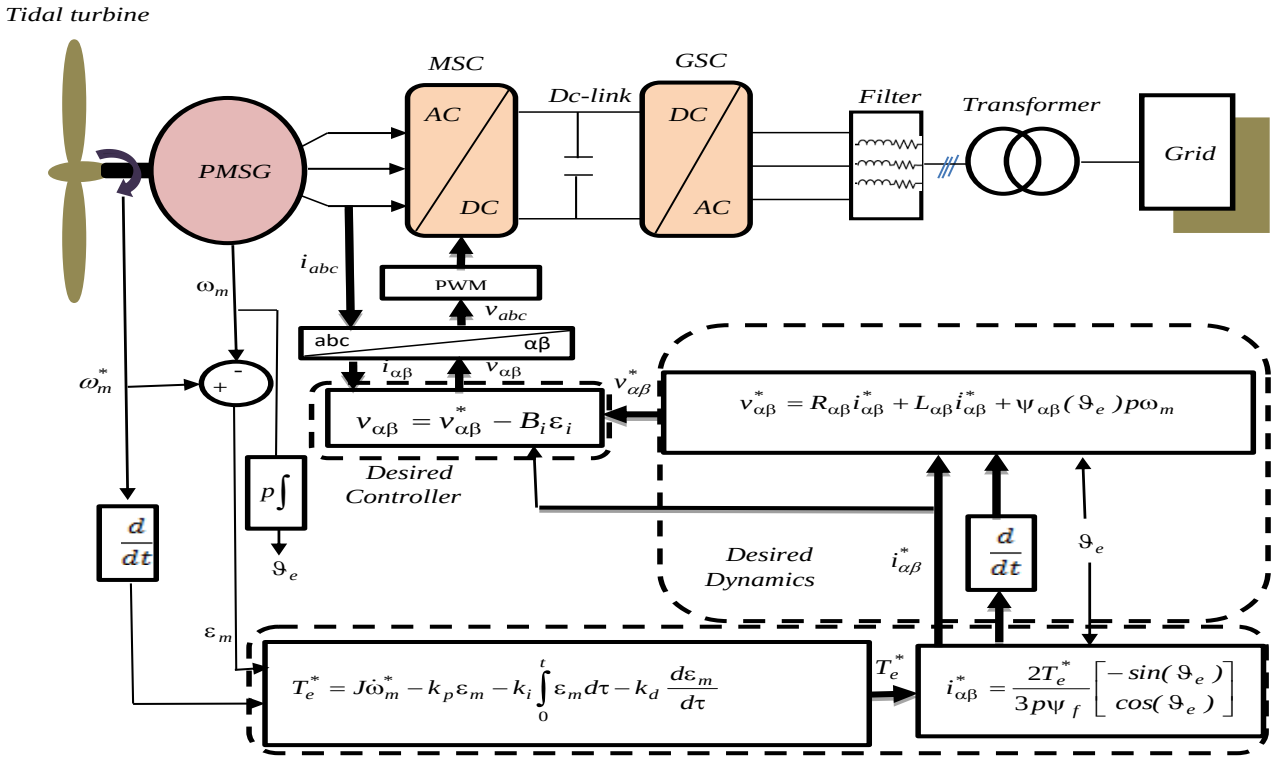

FIGURE III.1 The PBVC diagram.

The PMSG operate at an optimal speed if the desired is taken as [7]:

$$i_{\alpha\beta}^* = \frac{2T_e^*}{3p\psi_f}\begin{bmatrix}-\sin(\theta_e)\\ \cos(\theta_e)\end{bmatrix} \quad \text{(III.8)}$$

The desired torque is deduced from the mechanical dynamic equation (III.4), which is expressed by:

$$T_e^* = J\frac{d\omega_m^*}{dt} - f_{fv}(\omega_m^* - \omega_m) \quad \text{(III.9)}$$

The suitable dynamic is to minimize as much as possible the speed error between the PMSG and the marine current turbine. As can be seen from the above Eq. (III.9), the desired torque T_e^* has two drawbacks: its convergence depends on the PMSG mechanical parameters (J, f_{fv}) and it is in open loop [15]. To overcome that inconvenient, a PID controller is adopted by the PBVC design in

order to eliminate the static error, guarantee a fast convergence of the speed error $\varepsilon_m = (\omega_m^* - \omega_m)$, and ensure a robustness under different operation conditions. Thus, T_e^* is calculated as:

$$T_e^* = J\frac{d\omega_m^*}{d\tau} - k_p\varepsilon_m - k_i\int_0^t \varepsilon_m\, d\tau - k_d\frac{d\varepsilon_m}{d\tau} \quad \text{(III.10)}$$

Where, k_p>0, k_i>0, and k_d>0.

Remark 2. The speed and current errors convergence are ensured by the different internal and external loops of the proposed control in Figure 1, where the PID controller in the desired torque expression (Eq. (III.10)) imposes the desired currents (Eq. (III.8)) and ensure the convergence of the speed error, while the robustness of the PBVC and convergence of all errors are assured by the damping term "$B_i\varepsilon_i$" in the voltage $v_{\alpha\beta}$ (Eq. (III.7)). The condition expressed by Eq. (III.5) ensures a negative time derivative of the function $V_f^*(\varepsilon_i)$ (Eq. (III.6)), which ensures the stability of the closed loop system.

3 PI Controller of the GSC

There are many strategies used to control GSC [4, 17, 18]. In this study, the classical PI controller is adopted and applied to integrate the total generated active power from the MSC into the grid through the *DC*-Link when the reactive power is regulated at a predefined reference value. The dynamic model control of the GSC is represented in Figure III.2. The grid-side and *DC*-Link system equation in the *dq*-frame can be given as [17]:

$$\begin{bmatrix} v_{id} \\ v_{iq} \end{bmatrix} = R_f \begin{bmatrix} i_{df} \\ i_{qf} \end{bmatrix} + \begin{bmatrix} L_f\frac{di_{df}}{dt} - \omega L_f i_{qf} \\ L_f\frac{di_{qf}}{dt} + \omega L_f i_{df} \end{bmatrix} + \begin{bmatrix} v_{gd} \\ v_{gq} \end{bmatrix} \quad \text{(III.11)}$$

Where, v_{gd} and v_{gq} are the grid voltages, i_{df} and i_{qf} are the grid currents, v_{id}, v_{iq} denotes the inverter voltages, ω denotes the network angular frequency, R_f represents the filter resistance, and L_f is the filter inductance. The distributed network PI current controller contains two closed control. The inner, it consists to inject only the active power into the grid by enforcing quadrature current i_{qf} to zero, and the d-axis reference current i_{df} is determined by DC-bus voltage controller. While, the q-axis current i_{qf} is produced by the reactive power Q_g is the outer. The model of the DC voltage is [18]:

$$C\frac{dV_{dc}}{dt} = \frac{3}{2}\frac{v_{gd}}{V_{dc}}i_{df} + i_{dc} \tag{III.12}$$

Where, C denotes the DC-link capacitance, i_{dc} represents the grid side line current, and V_{dc} denotes the DC-link voltage. The current PI loop is given as:

$$\begin{cases} v_{gd}^{PI} = k_{gp}^{d}\left(i_{df}^{ref} - i_{df}\right) - k_{gi}^{d}\int_0^t\left(i_{df}^{ref} - i_{df}\right)d\tau \\ v_{gq}^{PI} = k_{gp}^{q}\left(i_{qf}^{ref} - i_{qf}\right) - k_{gi}^{q}\int_0^t\left(i_{qf}^{ref} - i_{qf}\right)d\tau \end{cases} \tag{III.13}$$

Where, $k_{gp}^{d} > 0$, $k_{gi}^{d} > 0$, $k_{gp}^{q} > 0$, $k_{gi}^{q} > 0$. The q-axis current i_{qf}^{ref} PI is expressed by:

$$i_{qf}^{ref} = k_{dcp}\left(V_{dc\_ref} - V_{dc}\right) - k_{dci}\int_0^t\left(V_{dc\_ref} - V_{dc}\right)d\tau \tag{III.14}$$

Where, $k_{dcp} > 0$ and $k_{dci} > 0$. Finally, the reactive power and active power are given by:

$$\begin{cases} \mathrm{P_g} = \frac{3}{2}\mathrm{v_{gd}i_{df}} \\ \mathrm{Q_g} = \frac{3}{2}\mathrm{v_{gd}i_{qf}} \end{cases} \tag{III.15}$$

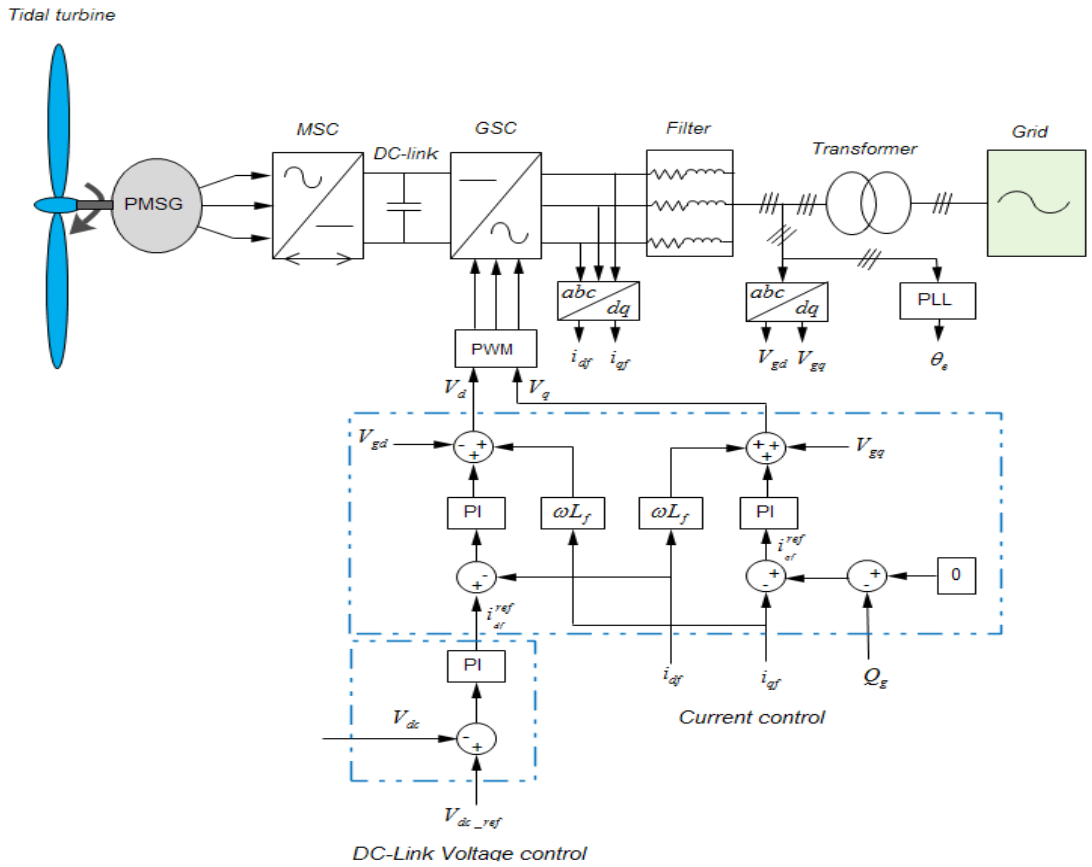

FIGURE III.2 Classical PI control schema.

4 Numerical validation

To evaluate the fusibility and performance of the proposed passivity-based voltage control (PBVC), extensive simulations under MATLAB/Simulink has been performed on a tidal turbine associated to a 1.5 MW, 125 rpm rated PMSG. The DC-link reference is set to 1150V and the reference reactive power fixed to zero. The overall tidal conversion system parameters are listed in Table 1 in Appendix B. The initial conditions used in simulation are: $[\omega_m(0), i_{dq}(0)] = [0,0,0]$ for the PMSG, Vdc(0) = 0 and $i_{daf}(0) = [0,0]$ for the grid. From the imposed pole location, the gains of the DC-link PI are $k_{dcp} = 5$ and $k_{dci} = 500$. The PBVC-PID controller gains are $k_p = 5$, and $k_i = 100$, and $k_d = 0.5$. The GSC current PI controller gains are $k_{gp}^d = k_{gp}^q = 9$, $k_{gi}^d = k_{gi}^q = 200$. Three scenarios are carried out in the simulation tests. The first one deals with the performances of the control strategies to the fixed parameter values. The second situation is assessing robustness of the developed strategy in regards to disturbances and parameter uncertainties. To verify the performances against parameter changes, three tests are carried out in this part. First, +50% and +100% stator resistance $R_s$variations are provoked. Second, a change of +50% and +100% of the total inertia J. Finally, simultaneous variations of +100% $R_s$and +100% J are performed. For the last scenario, a comparison of the robustness performance of the proposed strategy, SMC and the PI against parameter changes is performed.

4.1 Controller performance under fixed parameters

Figure III.3, show the dynamic of the used tidal speed. In Figure III.4, is represented the pace of the electromagnetic torque where the established regime is stabilized. It should also mentioned that during the steady-state, the torque remains constant without any fluctuation when using the proposed control. Figure III.5, shows the DC-link voltage response, here also, the proposed control results in a faster tracking of the reference value (1150V). As shown in Figure III.6, the reactive power is well kept at its zero-reference value. This is also confirmed this figure, which one can see that only the active power is transmitted to the grid. In summary, under fixed parameters, the proposed PBVC has successfully achieved the control objectives.

4.2 Proposed controller performance under parameter changes

Case 1: Stator resistance R_s variations

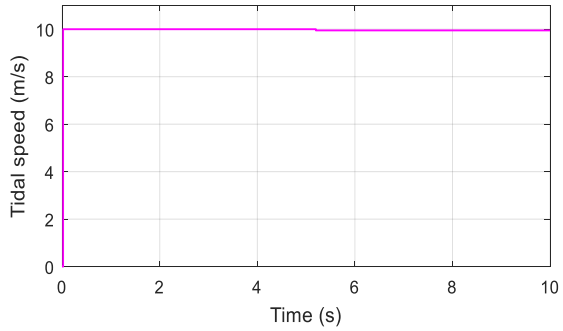

FIGURE III.3 Tidal speed.

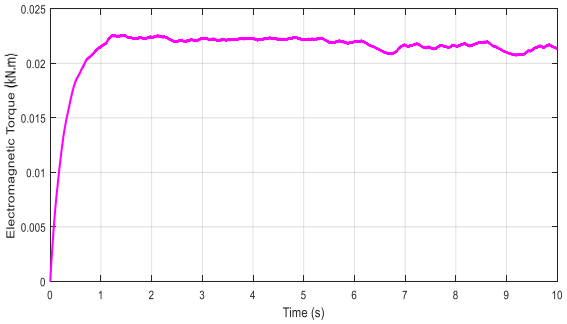

FIGURE III.4 Electromagnetic torque.

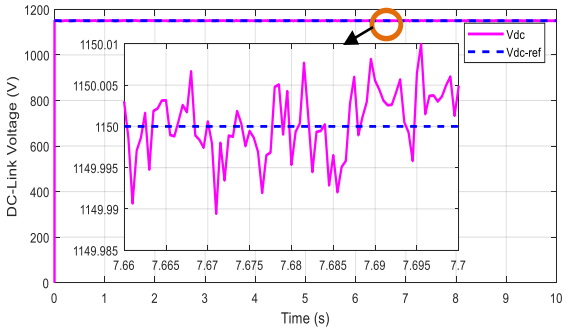

FIGURE III.5 DC-link voltage.

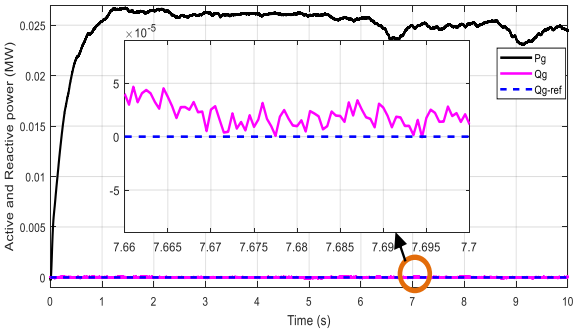

FIGURE III.6 Active and Reactive power.

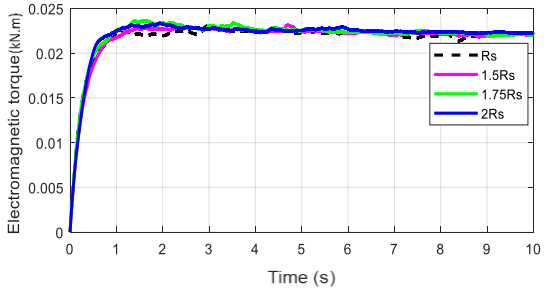

FIGURE III.7 Electromagnetic torque in with change of +50%, +75%, +100% of Rs.

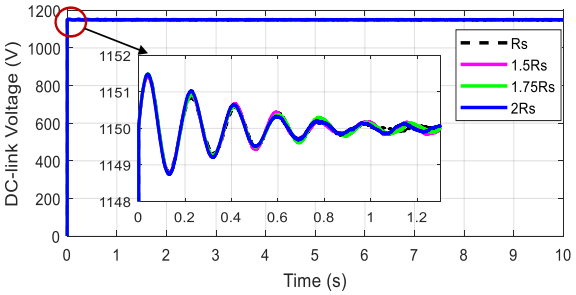

FIGURE III.8 DC-link voltage with change of +50%, +75%, +100% of Rs.

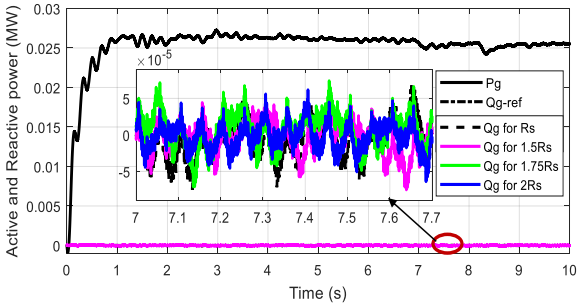

FIGURE III.9 Active and Reactive power in with change of +50%, +75%, +100% of Rs.

In Figure III.7, it can be seen that a variation of +50%, 75% and +100% of R_s does not influence the dynamic of the electromagnetic torque. The same remark can be made for the DC-link voltage shown in Figure III.8. No effect of resistance change on the reactive power and the

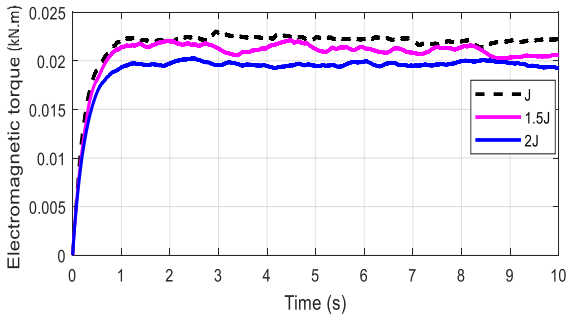

FIGURE III.10 Electromagnetic torque with change of +50 and +100% of J.

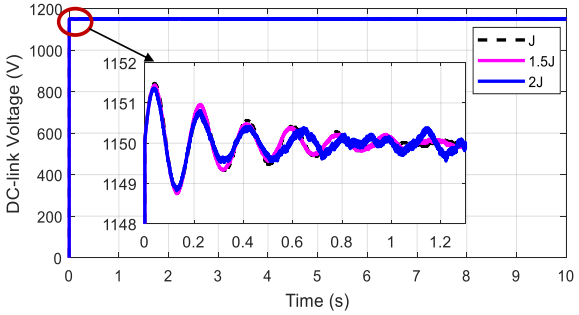

FIGURE III.11 DC-link voltage with change of +50% and +100% of J.

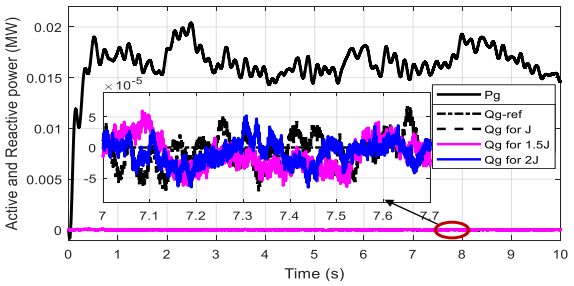

FIGURE III.12 Active and Reactive power with change of +50% and +100% of J.

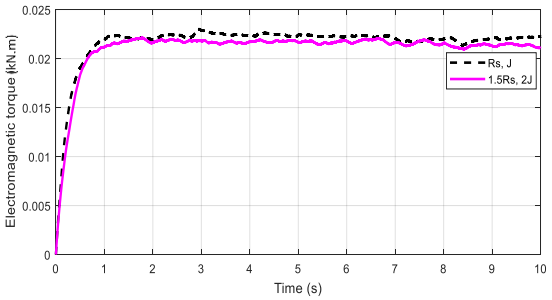

FIGURE III.13 Electromagnetic torque with change of +50% and +100% of J.

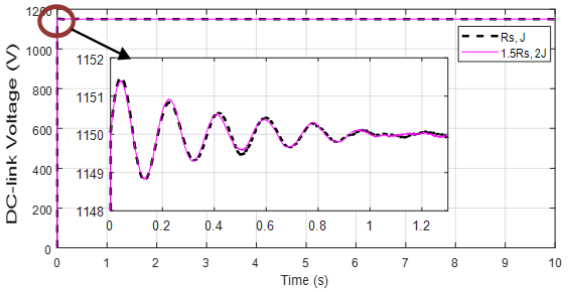

FIGURE III.14 DC-link voltage with change of +50% and +100% of J.

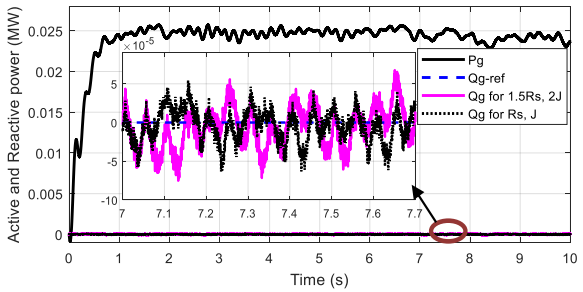

FIGURE III.15 Active and Reactive power (pu) with change of +50% and +100% of J.

active power is also observed in Figure III.9. On can conclude after this test, that the proposed control firmly resists against stator resistance changes.

Case 2: The total inertia J variations

From Figures III.10-III.12, it can be seen that the system under +50% and +100% changes in J, is slightly influenced by this perturbation on the performance of the system. This is due to the PBC design which based on the electrical part has no compensation between the electrical part and the mechanical part.

Case 3: simultaneous change R_s and J.

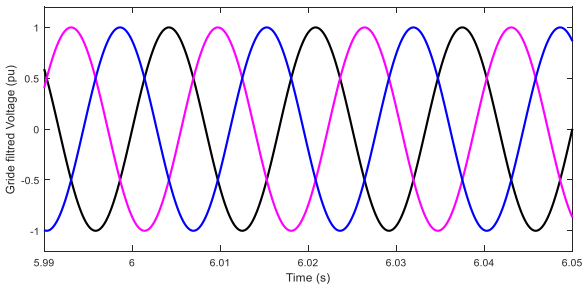

FIGURE III.16 Grid voltage.

The simultaneous +100% change of R_s and +100% of J, has no impact on the dynamic of the system as shown in Figures III.13-III.15, which show similar response as in the case 1.

Finally, for the three above tests, the robustness property of the proposed PBVC is interpreted as follow: for the first test, the system dynamic is not influenced by R_s due to the fact that the resistance variations are compensated by the imposed damping gain b_i in the PBVC design, (see Eq. (III.3)). The control robustness is ensured when that damping factor is chosen larger than R_s. Concerning the second test, the robustness sensitivity against the change of the inertia moment J is due to the desired torque (Eq. (III.10)) computed by the PID controller adopted by the PBVC which is still influenced by the inertia moment. For the simultaneous variations, the obtained performances are due to the large values of the gains of the dissipation term that compensate the error convergence as well as the parametric uncertainties. Finally, Figure III.16, show that the proposed control respects the power quality requirement with a perfect sinusoidal grid voltage absorption without overshoot.

5 Conclusion

In this chapter a novel passivity-based voltage controller (PBVC) for a permanent magnet synchronous generator-based tidal turbine conversion system is developed. The methodology for the proposed controller applied to PMSG has been illustrated. The simulation results performed using MATLAB/Simulink environment with the inclusion of the dynamics of the PMSG for a used tidal speed, show the effectiveness of the conversion system. The developed control strategy, shows the fast-tracking of the maximum tidal power harnessed, the reactive power generated and the DC-link quickly track their set values with an extremely minimized error. The objectives of the chapter are very well achieved. The PMSG-based conversion system provides a higher performance, robustness against generator parameter uncertainties, and efficiency. The control

strategy is reasonable, relatively simple structure, and is highly promising in marine current energy applications.

References

[1] Saini G, Saini RP. A review on technology, configurations, and performance of cross-flow hydrokinetic turbines. Int. J. Energy Res., 2019; 43: 6639-6679.

[2] Belkhier Y, Achour AY. Passivity-based voltage controller for tidal energy conversion system with permanent magnet synchronous generator. International Journal of Control, Automation and Systems, 2020; 19: 1-11.

[3] Othman AM. Enhancement of tidal generators by superconducting energy storage and jaya-based sliding-mode controller. International Journal of Energy Research, 2020; 44(14): 11658-11675.

[4] Gu Y-j, Yin X-x, Liu H-w, Li W, Lin Y-g. Fuzzy terminal sliding mode control for extracting maximum marine current energy. Energy, 2015; 90(1): 258-265.

[5] Zhou Z, Elghali BS, Benbouzid MEH, Amirat Y, Elbouchikhi E, Feld G. Tidal stream turbine control: An active disturbance rejection control approach. Ocean Engineering, 2020; 202: 107190.

[6] Toumi S, Elbouchikhi E, Amirat Y, Benbouzid M, Feld G. Magnet failure-resilient control of a direct-drive tidal turbine. Ocean Engineering, 2019; 187: 106207.

[7] Achour AY, Mendil B. Passivity Based Voltage Controller-Observer Design with unknown load disturbance for Permanent Magnet Synchronous Motor. 2014 IEEE 23rd International Symposium on Industrial Electronics (ISIE), 2014; 201-206.

[8] Nicklasson PJ, Ortega R, Pérez GE. Passivity-based control of the general rotating electrical machine. Proceeding of the 33rd Conference on Decision and Control. Lake Buena Vista, FL, 1994: 4018-4023.

[9] Pérez GE, Alcantar MG, Ramérez GG. Passivity-based control of synchronous generators. Proceeding of the IEEE International Symposium on Industrial Electronics (ISIE '97), 1997; 1: 101-106.

[10] Yang B, Yu H, Zhang Y, Chen J, Sang Y, Jing L. Passivity-based sliding-mode control design for optimal power extraction of a PMSG based variable speed wind turbine. Renewable Energy, 2018; 119: 577-589.

[11] Santos GV, Cupertino AF, Mendes VF, Junior SIS. Interconnection and damping assignment passivity-based control of a PMSG based wind turbine. IEEE 13th Brazilian Power Electronics Conference and 1st Southern Power Electronics Conference (COBEP/SPEC), Fortaleza, Brazil, 2015.

[12] David FM, Ortega R. Adaptive passivity-based control for maximum power extraction of stand-alone windmill systems. Control Engineering Practice, 2012; 20(2): 173-181.

[13] Yang B, Yu T, Shu H, Qiu D, Zhang Y, Cao P, Jiang L. Passivity-based linear feedback control of permanent magnetic synchronous generator-based wind energy conversion system: design and analysis. IET Renewable Power Generation. 2018; 12(9): 981-991.

[14] Fantino R, Solsona J, Busada C. Nonlinear observer-based control for PMSG wind turbine. Energy, 2016; 13: 248-257.

[15] Achour AY, Mendil B, Bacha S, Munteanu I. Passivity-based current controller design for a permanent-magnet synchronous motor. ISA Transactions, 2009; 48(3): 336-346.

[16] Jain B, Jain S, Nema RK. Control strategies of grid interfaced wind energy conversion system: An overview. Renewable and Sustainable Energy Reviews, 2015; 47: 983-996.

[17] Belkhier Y, Achour AY. An intelligent passivity-based backstepping approach for optimal control for grid-connecting permanent magnet synchronous generator-based tidal conversion system. Int. J. Energy Res., 2020: 1-16. DOI: 10.1002/er.6171.

[18] Errami Y, Ouassaid M, Maaroufi M. A performance comparison of a nonlinear and a linear

control for grid connected PMSG wind energy conversion system. Electrical Power and Energy Systems, 2015; 68: 180-194.

Chapter IV

Fuzzy passivity-based linear feedback current control approach for PMSG-based tidal turbine

1 Introduction

Recently, a large part of the control methods that are inspired from the wind technologies are in the development or testing phase, and the reference technology has not yet clearly established [1]. This work is motivated by the fact of controlling the PMSG without neglecting its mechanical part or removing it, to make it work at an optimal point. The key challenge, is the maintaining of the DC-link voltage and the reactive power to their reference values, whatever the disturbances related to nonlinear properties of the PMSG and its parameters which can vary significantly from their nominal values. With an important advantage of being an energy-based approach, in this chapter, a new passivity-based controller (PBC) which forces the PMSG to operate at an optimal torque and track time-varying speed of the tidal turbine is developed. The PBC was introduced to define a controller design methodology that achieves stabilization by reshaping the natural energy of the system and inject the required damping term. The main objective is to bring the system to a desired dynamic, without canceling the nonlinear dynamics and avoid introducing singularities in the closed-loop [2].

This proposed method is related to previous work [1] concerning the current control of a permanent magnet synchronous motor (PMSM), where the objective is the control of the PMSM, the mechanical torque Tm in equation (7) is estimated, but in our work, the PBC is used to control the permanent magnet synchronous generator (PMSG), where the mechanical torque Tm is generated by the tidal turbine which is a useful input for the PMSG. Also, the speed imposed on the PMSG is that of the tidal turbine which requires an adaptation of the control law. So, in order to much this adaptation, we operated an important modification on that proposed passivity-based current controller, a linear feedback is applied to the PMSG model that allows the maintaining of the armature reaction flux in quadrature with the rotor flux which introduces a fast-internal loop that decouples the variables from the PMSG, this leads to simple control structure and simple mathematical calculation, and allows the PBC to be faster and more efficient. Also, a fuzzy logic controller is adopted to design the desired torque dynamic to guarantee a fast convergence, stability, and robustness against parameter variations of the controlled system. In the proposed method, the dynamic of the PMSG were represented as feedback interconnection of a passive electrical and mechanical subsystem. The PBC is applied only to the electrical subsystem while the mechanical subsystem has been treated as a passive perturbation. The use of the PMSG dq-model

in the computation of the PBC avoids the model structure destruction due to singularities, since dq-model does not depend explicitly on the rotor angular position. The PBC is an energy-based approach therefore the dependence of the controller on system parameters is extremely reduced and avoids the cancellation of non-linearities of the system. Then, the dynamic response is fast, efficient, the asymptotic stability and the robustness of the conversion system are improved.

An up-to-date of the development and the newest achievement in large marine current turbine technologies from 500 kw to 2 MW have been reported by [2]. The authors have provided an important background for researchers in tidal energy domain, all types of the tidal turbines have been investigated. In order to achieve the maximum power extraction under large parametric nonlinearities and uncertainties of a new hydrostatic tidal turbine, in [3], a nonlinear predictive controller that uses short-term predictions of the approaching tidal speed field when is below the rated value to enhance the maximum tidal power generations. An integral action is incorporated into the control loop and a nonlinear observer-based smooth second order sliding mode control to improve the robustness against parameter variations and uncertainties. The same system is also investigated in [4], in that work, a nonlinear observer-based extreme learning machine is proposed, associated to a sliding mode control and compared to the conventional PID control, which showed that the proposed control systems achieved much better performance than the conventional one. However, as mentioned in [5], the aforementioned strategies are signal-based and a large part of them usually neglect the physical properties of the PMSG during the controller computation. The proposed controller is compared to conventional approaches, such as second-order sliding mode control [6], and PI-control [7]. The proposed fuzzy-PBC has the following advantages: It presents simple structure and mathematical calculation, it shows a fast convergence and guarantees stability considering the nonlinear model of the system and it provides a higher robustness again parameter variations.

2 Passivity-based control theory and design procedure

The controller objective is to forces the PMSG to track the tidal turbine speed. The first step of our design procedure, is the decomposition of the PMSG model into the feedback interconnection of two passive subsystems, its electrical and mechanical dynamics, where the latter can be treated as a "passive disturbance". We design then a PBC for the electrical subsystem and a damping term is injected to make the electrical subsystem strictly passive, which forces the PMSG to track

velocity. The design procedure of the passivity-based current control with linear feedback applied to the MSC is represented by the Figure IV.1, it consists in tow main parts: the desired dynamics described as the reference current and the reference electromagnetic torque and then, calculating the control voltage [8].

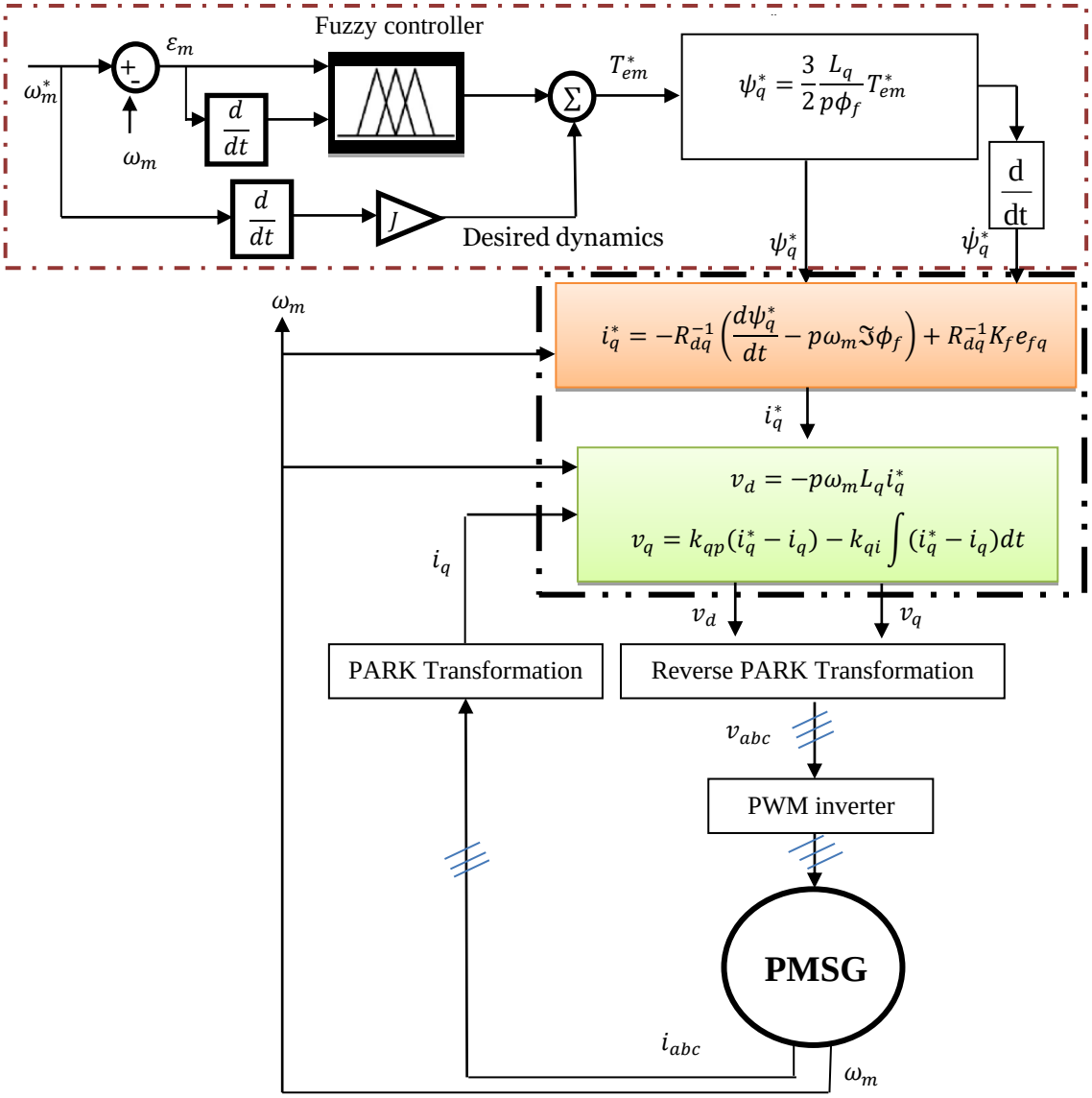

FIGURE IV.1 Proposed passivity control block diagram.

2.1 Linear feedback current-controlled dq-model of the PMSG

The interdependence between the flux linkage ψ_{dq} and the current vector i_{dq} can be expressed as follow:

$$\psi_{dq} = \begin{bmatrix} \psi_d \\ \psi_q \end{bmatrix} = \begin{bmatrix} L_d i_d + \psi_f \\ L_q i_q \end{bmatrix} \quad \text{(IV.1)}$$

Substituting the i_{dq} expression obtained from (IV.1) in (I.7) yields:

$$v_{dq} - R_{dq} i_{dq} = \frac{d\psi_{dq}}{dt} + p\omega_m \Im \psi_{dq} \quad \text{(IV.2)}$$

Before calculating the PBC, we will apply to the PMSG a nonlinear feedback which allows maintaining the armature reaction flux in quadrature with the rotor flux. This flux orientation control will enforce the d-axis current i_d to zero and the behavior of the PMSG will be similar to that of a DC-generator, so this control method has a linearizing feedback.

The equation that expresses this linearizing feedback is given as:

$$v_d = -p\omega_m L_q i_q \quad \text{(IV.3)}$$

The application of the relation (IV.1) to the model (IV.2) imposes a zero i_d current and we get then the following simplified model:

$$v_q - R_s i_q = \frac{d\psi_q}{dt} - p\omega_m \Im \psi_q \quad \text{(IV.4)}$$

The proportional-integral (PI) loop which forces the quadrature current i_q to track the reference value i_q^* is:

$$v_q = k_{qp}\left(i_q^* - i_q\right) + k_{qi} \int_0^t (i_q^* - i_q) dt \quad \text{(IV.5)}$$

Then, the PMSG model decoupled by the oriented flux control given below is controlled by the input i_q^* :

$$\frac{d\psi_q}{dt} - p\omega_m \psi_q = -R_s i_q^* \quad \text{(IV.6)}$$

$$J\frac{d\omega_m}{dt} = T_m - T_{em} - f_{fv}\omega_m \quad \text{(IV.7)}$$

$$T_{em} = -\frac{3}{2} p\phi_f i_q^* \quad \text{(IV.8)}$$

The control input i_q^* is designed by the passivity approach, using the previous simplified model (IV.6)-(40).

2.2 Fuzzy passivity-based linear feedback controller structure of a PMSG

We consider the desired value of the flux linkage vector $\psi_{dq}^{*} = [\psi_{d}^{*} \quad \psi_{q}^{*}]^{T}$ and the vector of the tracking error is $e_f = [e_{fd} \quad e_{fq}]^{T} = \psi_{dq} - \psi_{dq}^{*}$. By replacing e_f in Eq. (IV.1), we deduce the dynamic equation of e_f. By considering the function $V(e_f) = 0.5 e_f^{T} e_f$ and by using the Lyapunov theory, we deduce the control signals $i_{dq}^{*} = [i_{d}^{*} \quad i_{q}^{*}]^{T}$ which ensure the convergence of the flux linkage tracking error e_f, given below:

$$\begin{cases} i_{d}^{*} = 0 \\ i_{q}^{*} = \frac{1}{R_s}\left(-\frac{d\psi_{q}^{*}}{dt} + p\omega_m\phi_f + K_{fq}e_{fq}\right) \end{cases} \quad \text{(IV.9)}$$

With $K_{fq} > 0$. The proof of exponential convergence and stability of the currents error, is given in Appendix A as is the same for the PMSG in the αβ-model.

2.3 Desired flux computation

The computation of the control signal i_{dq}^{*} requires the desired flux vector ψ_{dq}^{*}. If the direct current i_d is maintained equal to zero, then the PMSG operates under maximum torque. Under this condition, and using (IV.1), it results [1]:

$$\psi_{q}^{*} = L_q i_{q}^{*} \quad \text{(IV10)}$$

Therefore, the expression of the flux reference is deduced from (IV.8) and (IV.10) as:

$$\psi_{q}^{*} = \frac{2}{3}\frac{L_q}{p\phi_f} T_{em}^{*} \quad \text{(IV.11)}$$

where, T_{em}^{*} is the desired torque.

2.4 Desired torque computation using a fuzzy logic controller

From the mechanical dynamic Eq. (IV.8) and taking the rotor speed ω_m equal to its set-point, we compute the desired torque, which is given as follows:

$$T_{em}^{*} = J\frac{d\omega_{m}^{*}}{dt} - f_{fv}\omega_{m}^{*} + T_m \quad \text{(IV.12)}$$

Where, ω_{m}^{*} is the tidal turbine speed. As mentioned in chapter II, this expression of the desired torque T_{em}^{*} has two drawbacks: it is in an open loop and its convergence is limited by the mechanical parameters (J, f_{fv}) of the PMSG. In this work, we introduced a fuzzy logic controller to design the desired torque dynamic to eliminate the static error, stability, and robustness against

parameter variations of the closed-loop, and ensure the fast convergence of the speed tracking error $\varepsilon_m = \omega_m^* - \omega_m$. The fuzzy controller design procedure has three steps which are: fuzzification, rule base and defuzzification. Two inputs signals are considered for the fuzzy block, the speed error ε_m and its derivative. The membership function of the fuzzy controller inputs and outputs shown as two trapezoidal and three triangular groups type (see Figure IV.2). In Table II, we definite five fuzzy sets (linguistic variables) for the inputs and outputs of the fuzzy logic block to get the rule base, which are expressed as: Negative Big (NB), Negative Small (NS), Zero (Z), Positive Small (PS), Positive Big (PB). The defuzzification step is performed by using the center of gravity method. Then the desired torque is computed as expressed in Figure IV.3.

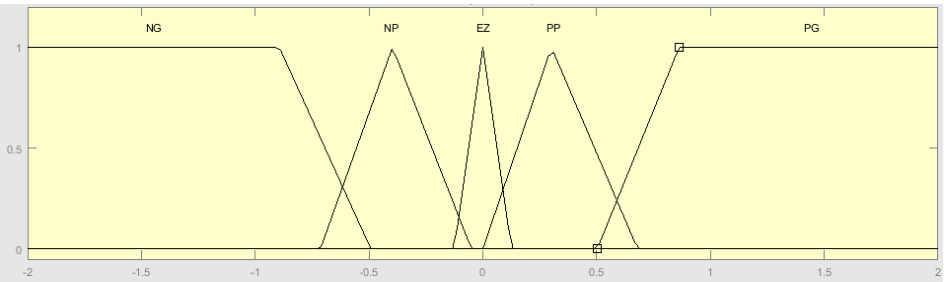

a. The membership function of the speed error ε_m.

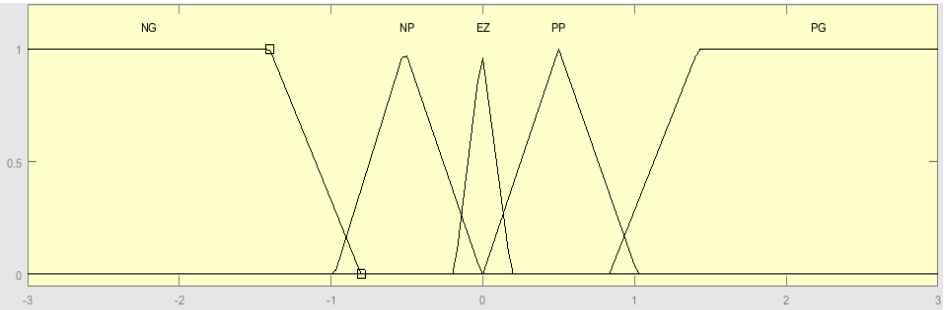

b. The membership function of the speed error variation $\Delta\varepsilon_m$.

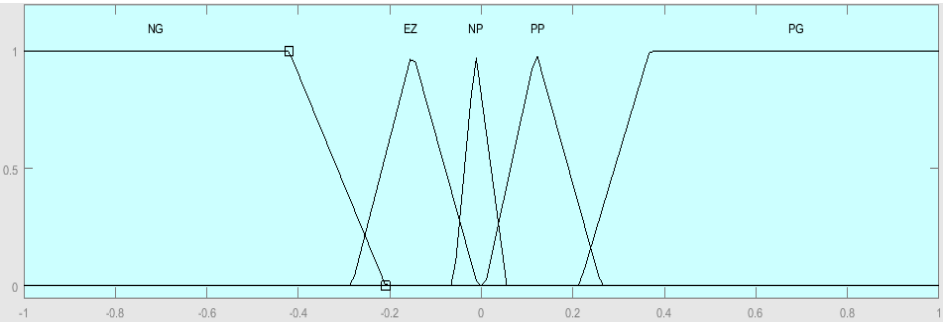

c. The membership function of the output of the fuzzy controller.

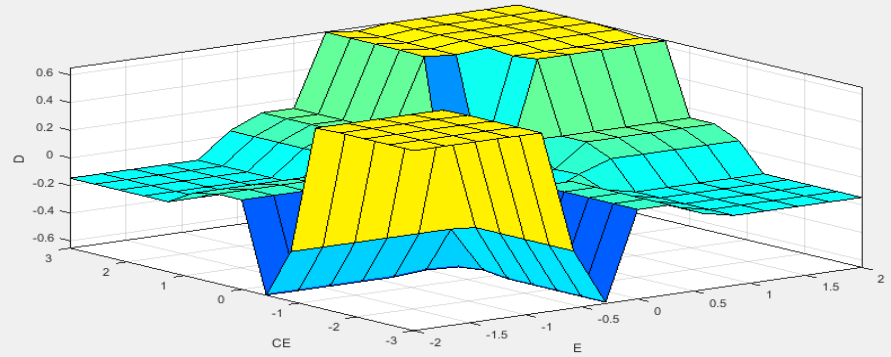

d. The fuzzy controller surface.

FIGURE IV.2 The fuzzy controller configuration.

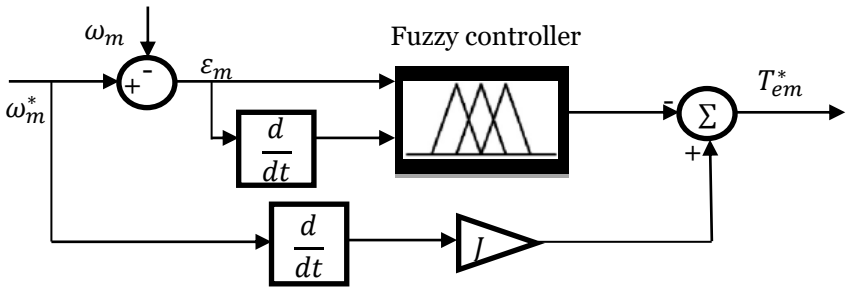

FIGURE IV.3 Desired torque computation using fuzzy logic controller**.**

TABLE II. Fuzzy logic rules.

ε_m \ $\Delta\varepsilon_m$	NB	NS	Z	PS	PB
NB	NB	NB	NS	NS	Z
NS	NB	NB	NS	Z	PS
Z	NS	NS	Z	PS	PS
PS	NS	Z	PS	PB	PB
PB	Z	PS	PS	PB	PB

3 Conventional PI controller of a PMSG

The PI controller used in this work, in order to compare the performances of the proposed PBC strategy, has two interdependent loops, the d-axis current loop, and the q-axis current loop, as illustrated in Figure I.10. The first loop aim is to fix at unity power factor by controlling the d-axis stator current i_d component and setting the desired d-axis stator current i_d^* to zero. The q-axis loop has the objective to control the generator speed and torque by computing the desired q-axis component of the stator current with a tidal turbine which is the reference speed and PMSG speed

tracking error [9]. The voltage controller components of the PMSG can be computed by the following expression

$$v_d = v_d^* - \omega_e L_q i_q \tag{IV.13}$$

$$v_q = v_d^* - \omega_e\left(L_d i_d + \phi_f\right) \tag{IV.14}$$

With,

$$v_d^* = k_{dp}^{PI}(i_d^* - i_d) - k_{di}^{PI}\int_0^t (i_d^* - i_d)d\tau \tag{IV.15}$$

$$v_q^* = k_{qp}^{PI}\left(i_q^* - i_q\right) - k_{qi}^{PI}\int_0^t \left(i_q^* - i_q\right)d\tau \tag{IV.16}$$

Where $k_{dp}^{PI} > 0$, k_{di}^{PI}, $k_{qp}^{PI} > 0$, $k_{qi}^{PI} > 0$, $\omega_e = p\omega_m$ and the desired current i_q^* is given by the following PI expression:

$$i_q^* = k_p(\omega_m^* - \omega_m) - k_i\int_0^t (\omega_m^* - \omega_m)d\tau \tag{IV.17}$$

Where $k_p > 0$ and $k_p > 0$.

4 Simulation results and observation

The proposed control structure of Figure IV.1, were performed using the simulated tidal conversion system illustrated on Figure I.8, under MATLAB/Simulink environment based on PMSG with rated power of 1.5MW and rated speed of 125rpm, the DC-link reference is set to 1150V and the reference reactive power is fixed to zero, in order to confirm the proposed method performances and reliability. The parameters used for the simulation of the conversion system are same as in chapter III (see Table I). From the pole placement method, The gains concerning the generator side and the grid side current PI controller are listed in Table III. The proposed fuzzy passivity-based linear feedback current (FPBLFC) controller will be compared to the conventional (PI) controller method. The simulation tests are divides into two scenarios, the first aspect shows the performance of the conversion system to the initial parameter values. The second scenario, concerns the robustness tests of the proposed control design against parameter changes and disturbances is carried out. Three cases are studied in this part. In the first case, a variation of +50% of the stator resistance value R_s is performed. For the second case, a variation +100% of the

total inertia J is simulated and the last test deal with the simultaneous variation of +50% R_s and +100% J. Concerning the PBC simulation, the parameter $k_{f\mathrm{q}} = 100$.

4.1 Performance of the proposed method under initial parameter values

Figure IV.4, illustrate the used tidal speed characteristics, with variation between 4 m/s and 8 m/s. Figure IV.5, show the DC-link voltage response, which indicates that the DC voltage under the FPBLFC method is very well maintained at its reference value 1150V, with an extremely fast convergence when compared to the PI response which present a slow convergence. Figure IV.6 and Figure IV.7, shows that only the active power is transmitted to the grid, while the reactive power is very well kept at its zero-reference value, as indicates that the reactive power is extremely minimized for both conventional and proposed control. However, as can be seen, the FPBLFC strategy present a fast convergence to the zero-reference then the conventional one. In Figure IV.8, it can be seen that the control operation achieves with a perfect sinusoidal grid voltage absorption without overshoot. In this part, the control objectives of the proposed method are very well achieved for the initial parameter conditions. The proposed FPBLFC method provides a best performance when compared to the conventional PI method. As demonstrated, the FPBLFC controller show a higher tracking error with a fast convergence of the DC-link voltage and the reactive power.

TABLE III CONTROLLER STRATEGIES GAINS VALUES

PI (MSC)		PI (GSC)		FPBLFC	
GAINS	VALUES	GAINS	VALUES	GAINS	VALUES
k_{dp}^{PI}	0.5	k_{gp}^{d}	9	k_{qp}	800
k_{di}^{PI}	50	k_{gi}^{d}	200	k_{qi}	50
k_{qp}^{PI}	0.5	k_{gp}^{q}	9		
k_{qi}^{PI}	50	k_{gi}^{q}	200		
k_p	5	k_{dcp}	5		
k_i	500	k_{dci}	500		

4.2 Performance of the proposed method under parameter changes

Case 1: a change of +50% of the stator resistance R_s

Due to the PMSG dynamical, the stator resistance is influenced by the temperature, consequently the stator currents dynamic becomes more aggressive. In Figure IV.9 and Figure IV.10, we can see that a change of +50% of the stator resistance does not influence the speed convergence of the FPBLFC strategy for all the DC-link voltage, and the reactive power responses,

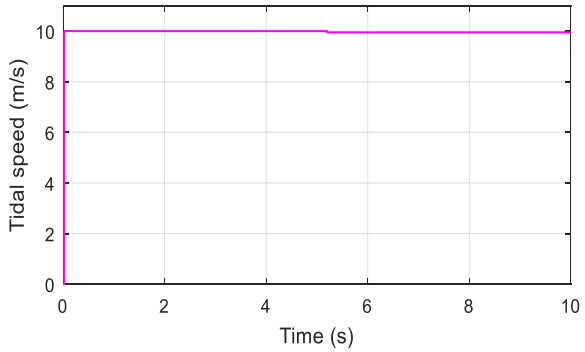

FIGURE IV.4 Tidal Speed.

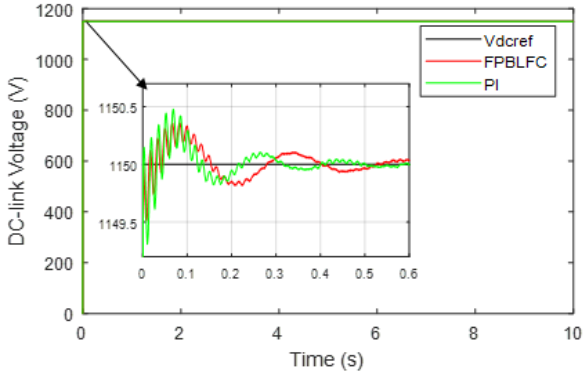

FIGURE IV.5 DC voltage.

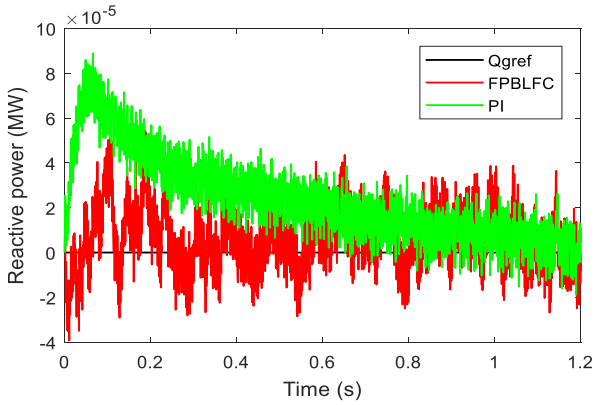

FIGURE IV.6 Generated Reactive power.

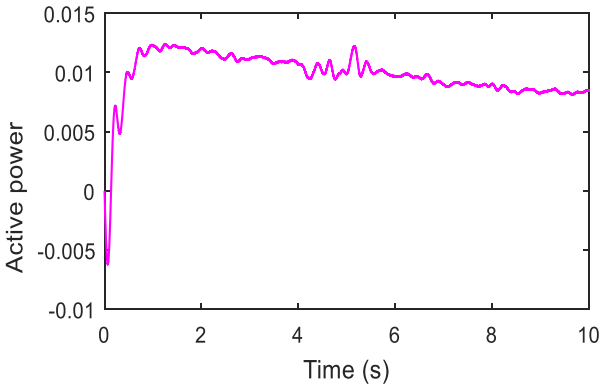

FIGURE IV.7 Generated Active power (pu).

when compared to the PI control, which its response present an increases of the convergence error due to the fixed gains that are very sensitive to parameter changes. This means that the proposed FPBLFC controller has remedied to the disturbance of the PMSG, this is due to the imposed damping gain k_{fq} appearing on the PBC design in Eq. (46), which compensated the variation. Because, it is these gain that ensure robustness if it is chosen large compared to R_s value.

Case 2: a change of +100% of the total inertia J

As can be seen in Figure IV.11 and Figure IV.12, a change of +100% of the inertia moment J, has no influence on the system performance. This is because the FPBLFC controller design illustrated in section 4, which is not influenced by the total moment J, due to the fuzzy controller of Figure IV.3, that has compensated the effect of J on the mechanical part. However, the conventional is also influenced by the variation of total moment for the same reason as in the previous case.

Case 3: a simultaneous variation of +50% of the stator resistance R_s and +100% of the total

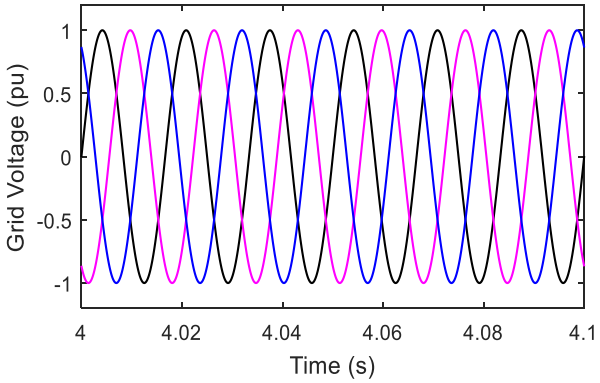

FIGURE IV.8 Generated voltage.

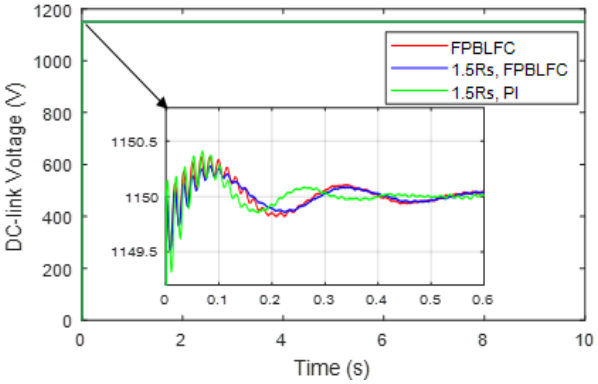

FIGURE IV.9 DC-link response for a change of +50% of stator resistance.

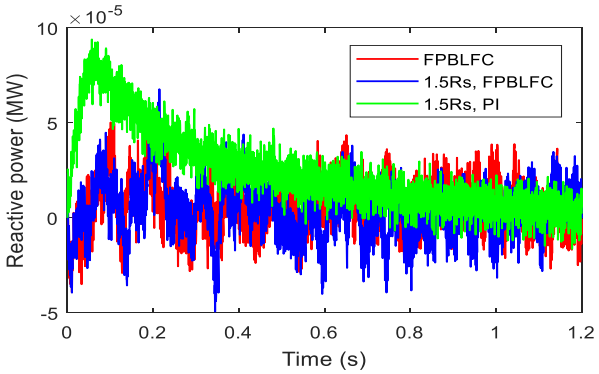

FIGURE IV.10 Reactive power response for a change of +50% of stator resistance.

inertia J

As indicated in Figure IV.13 and Figure IV.14, a simultaneous variation of +50% of the stator resistance R_s and +100% of the total inertia J, give a similar response concerning the proposed FPBLFC controller, as in the case 2, this is due to the procedure design of the PBC in section 2 and 3, which compensate the parametric uncertainties as well as the convergence of the pursuit errors which is assured, while the classical method which is impacted by simultaneous change.

4.3 Comparative analyse of the proposed method with the conventional PI controller

All tests performed in this section under the simulated conversion system platform, show clearly that the FPBLFC control strategy exhibits an efficient tracking speed. Furthermore, the FPBLFC controller present an extremely robustness performance against parameter changes compared to the classical PI controller. So, as depicted, the proposed control method has a higher effectiveness.

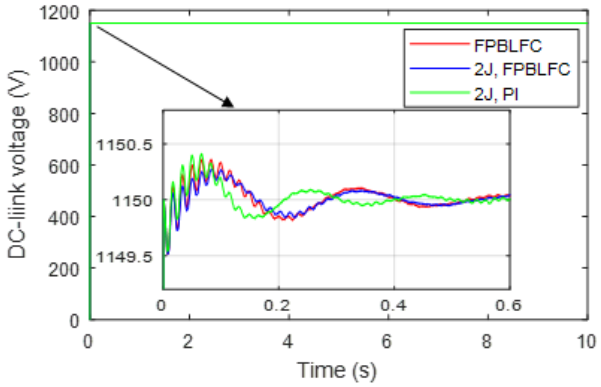

FIGURE IV.11 DC voltage response for a change of +100% of inertia moment.

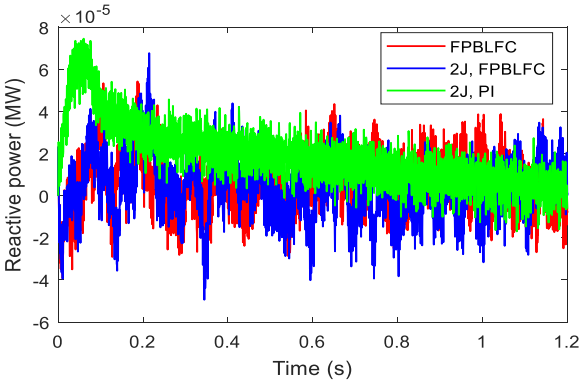

FIGURE IV.12 Reactive power response for a change of +100% of inertia moment.

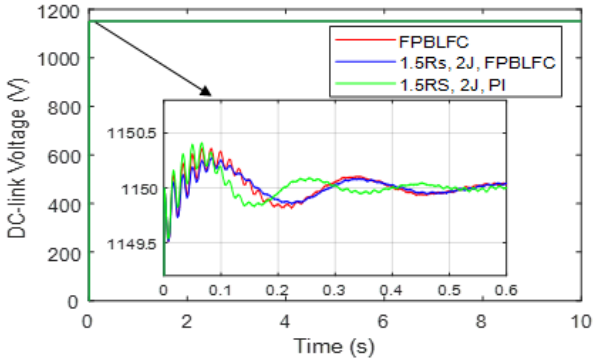

FIGURE IV.13 DC voltage response for simultaneous variation.

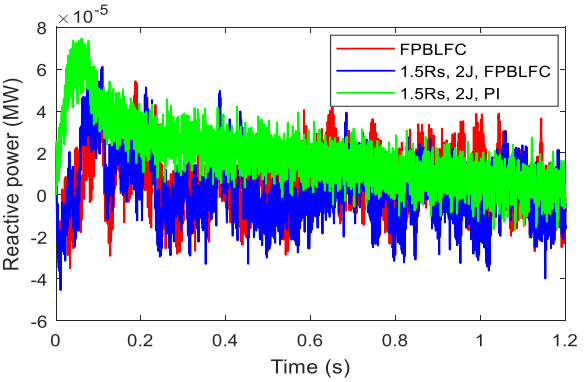

FIGURE IV.14 Reactive power response for simultaneous variation.

5 Conclusion

In this chapter, a new passivity-based control associated with a fuzzy logic controller for a tidal conversion system based PMSG, has been developed. The modeling and methodology for the proposed strategy applied to PMSG, has been described, analyzed and compared to the conventional PI controller. The simulation results show the effectiveness of the conversion system, with the inclusion of the dynamics of the PMSG.

The simulation studies under MATLAB/Simulink, show the fast-tracking of the maximum tidal power point, the DC-link is very well kept at its constant value and reactive power generated is extremely minimized with the proposed method. The control strategy is reasonable, simple structure, and is highly promising in tidal energy applications. The tidal conversion system-based PMSG provides a good performance, significant robustness against generator parameter uncertainties and efficiency.

References

[1] Achour, A. Y., Mendil, B., Bacha, S., Munteanu, I., 2009. Passivity-based current controller design for a permanent-magnet synchronous motor. ISA Transactions. 48(3), 336-346.

[2] Zhou, Z., Benbouzid, M. E. H., Charpentier, J. F., Scuiller, F., Tang, T., 2017. Developments in large marine current turbine technologies - A Review. Renewable and Sustainable Energy Reviews. 71, 852-858.

[3] Yin, X., Zhao, X., 2019. ADV Preview based nonlinear predictive control for maximizing power generation of a tidal turbine with hydrostatic transmission. IEEE Transactions on Energy Conversion. 34(4), 1781-1791.

[4] Yin, X., Zhao, X., 2020. Sensorless maximum power extraction control of a hydrostatic tidal turbine based on adaptive extreme learning machine. IEEE Transaction on Sustainable Energy. 11(1), 426-435.

[5] Yang, B., Wu, Q. H., Tiang, L., Smith, J. S., 2013. Adaptive passivity-based control of a TCSC for the power system damping improvement of a PMSG based offshore wind farm. IEEE International Conference on Renewable Energy Research and Applications ICRERA-2013, Madrid, Spain, 1-5.

[6] Benelghali, S., Benbouzid, M. E. H., Charpentier, J. F., et al., 2011. Experimental validation of a marine current turbine simulator: application to a permanent magnet synchronous generator-based system second-order sliding mode control. IEEE Trans. Ind. Electron. 58(1), 118-126.

[7] Zhou, Z., Scuiller, F., Charpentier, J. F., Benbouzid, M. E. H., Tang, T., 2013. Power smoothing control in a grid-connected marine current turbine system for compensating swell effect. IEEE Transaction on Sustainable Energy. 4(3), 816-826.

[8] Belkhier, Y., Achour, A. Y., 2020. Fuzzy passivity-based linear feedback current controller approach for PMSG-based tidal turbine. Ocean Engineering, 218.

[9] Khefifi, N., Houari, A., Machmoum, M., Ghanes, M., Ait-Ahmed, M., 2019. Control of grid forming inverter based on robust IDA-PBC for power quality enhancement. Sustainable Energy, Grids and Networks. 20, 100276.

Chapter V

An intelligent passivity-based backstepping approach for optimal control for grid-connected permanent magnet synchronous generator-based tidal conversion system

1 Introduction

In this chapter, a new control strategy, that uses a passivity theory is proposed. As mentioned previously, the inherent advantages of controller based on passivity theory are the guaranteed stability, the compensation of the nonlinear terms not by cancellation but in a damped way, and enhanced robustness properties, that forces the PMSG to track the time-varying speed of the tidal turbine and operate at an optimal torque. A methodology is introduced to define a controller design that achieves stabilization by reshaping the natural energy of the system and inject the required damping term [1]. This chapter proposes a new adaptive fuzzy linear feedback passivity-based backstepping controller (AFL-PBBC) to solve the problems related to the PMSG. The main objectives of this chapter are same as in the previous chapters which is controlling the PMSG without neglecting its mechanical part or removing it to make it work at an optimal point, the DC voltage and the reactive power must be maintained at their set values whatever the disturbances related to the PMSG. To improve the performance of the conversion system, special attention is made to the robustness against parameter variations. The first step of our design procedure is also the same as in chapter 4 which is the decomposition of the PMSG model into feedback interconnection of two passive subsystems, its electrical and mechanical dynamics, where the latter can be treated as a "passive disturbance". Then, the proposed new passivity-based control is designed for the electrical subsystem. The contribution Novel adaptive fuzzy linear feedback passivity-based backstepping controller is proposed and applied to a PMSG in the tidal conversion system. A linear feedback is applied to the PMSG model that allows the maintain of the armature reaction flux in quadrature with respect to the rotor flux, introducing therefore a fast-internal loop that decouples the PMSG variables. This leads to simpler control structure and easy mathematical calculation, and then faster and more efficient PBC. A fuzzy logic controller is associated with the PBC to design the desired torque dynamic, in order to accommodat the nonlinear operation of the PMSG which is the control structure proposed in chapter 4. The improvement which has been apported in this chapter is that the proposed controller in chapter 4 is combined with a backstepping controller to design a hybrid control law, while the stator resistance value is adapted to overcome its variations due to the temperature, which increases the robustness of the system. In fact, due to the designed PBC in chapter 3 that has no direct compensation between the electrical and the mechanical parts [2]. The

stator resistance that appears in the expression of the control vector v_{dq} is affected by the temperature, requiring therefore to be adapted.

2 Proposed PMSG controller design

The design of the AFL-PBBC applied to the MSC requires the following steps: the desired torque computed by the fuzzy logic controller and the desired currents that are described as the desired dynamics and the desired voltage designed by the backstepping controller as the control law as shown in Figure V.1.

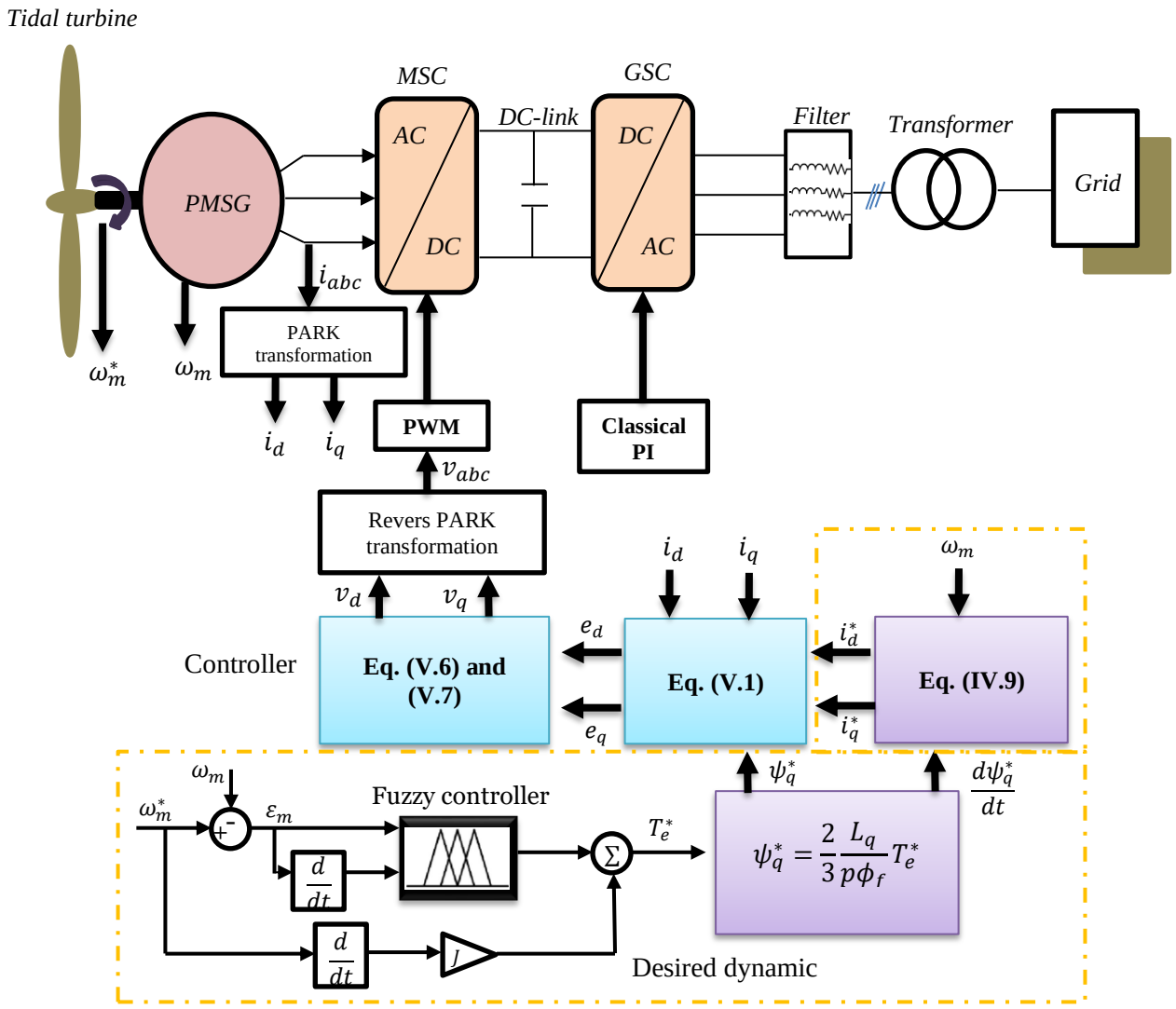

FIGURE V.1 Proposed passivity controller design.

3 Control law of the PMSG using Backstepping

In the backstepping controller design, it is aimed to transform the system and make it a first-order cascade subsystem [3]. The voltage controller v_{dq} which is the controller output of the PMSG is computed by using the Backstepping control, to allow the PMSG to operate at the same speed with the marine current turbine by generating a stabilizing function. The current controller i_{dq}^{*} computed with the linear feedback passivity-based control expressed by (IV.14), can be considered as the current reference components of the backstepping controller to release the stabilizing function. Then, we define the current tracking errors given by [4]:

$$e_{dq} = \begin{bmatrix} e_d \\ e_q \end{bmatrix} = \begin{bmatrix} i_d^* - i_d \\ i_q^* - i_q \end{bmatrix} \tag{V.1}$$

From (I.11), (IV.9) and (V.1), the derivative of current tracking errors is computed as follow:

$$\frac{de_{dq}}{dt} = \begin{bmatrix} \frac{di_d^*}{dt} - \frac{di_d}{dt} \\ \frac{di_q^*}{dt} - \frac{di_q}{dt} \end{bmatrix} =$$

$$\begin{bmatrix} \frac{R_s}{L_d} i_d - \frac{p\omega_m L_q}{L_d} i_q - \frac{v_d}{L_d} \\ R_s^{-1} \frac{d}{dt}\left(\left(-\frac{d\psi_q^*}{dt} + p\omega_m \phi_f\right) + K_f e_\psi\right) - \left(-\frac{R_s}{L_q} + \frac{p\omega_m L_d i_d}{L_q} - \frac{p\phi_f \omega_m}{L_q} - \frac{v_q}{L_q}\right) \end{bmatrix} \tag{V.2}$$

To compute the stator voltage controller v_{dq}, we define the following Lyapunov function:

$$V = \frac{1}{2}\left(e_d^2 + e_q^2\right) \tag{V.3}$$

The derivative of (V.3) yields:

$$\dot{V} = e_d \frac{de_d}{dt} + e_q \frac{de_q}{dt} = -k_1 e_d^2 - k_2 e_q^2 + e_d \left(\frac{R_s}{L_d} i_d - \frac{p\omega_m L_q}{L_d} i_q - \frac{v_d}{L_d} + k_1 e_d\right)$$

$$+ e_q \left(\frac{R_s}{R_s + K_f L_d}\left[-R_s^{-1}\dot{\psi}_q^* + \omega_m p\phi_f \left(\frac{f_{fv}}{JR_s} + \frac{1}{L_q}\right) + i_q \left(\frac{R_s}{L_q} - \frac{(p\phi_f)^2}{JR_s}\right) + \frac{p\phi_f}{JR_s} T_m - \frac{v_d}{L_d} + k_2 e_d \frac{R_s + K_f L_d}{R_s}\right]\right) \tag{V.4}$$

Finally, we get:

$$\dot{V} = -k_1 e_d^2 - k_2 e_q^2 < 0 \tag{V.5}$$

Where, $k_1 > 0$ and $k_2 > 0$. The equation (V.5) guarantees the overall asymptotic stability of the system only if the voltage components v_{dq} in Eqs. (IV.3) and (IV.5) are chosen as follow:

$$v_d = R_s i_d - p\omega_m L_q i_q + k_1 L_d e_d \tag{V.6}$$

$$v_q = L_q R_s^{-1}\dot{\psi}_q^* + \omega_m p\phi_f\left(\frac{L_q f_{fv}}{JR_s} + 1\right) + i_q\left(R_s - \frac{L_q(p\phi_f)^2}{JR_s}\right) + \frac{L_q p\phi_f}{JR_s}T_m + L_q e_d\frac{R_s + K_f L_d}{R_s} \tag{V.7}$$

The convergence of current errors is ensured by the different internal and external loops in the proposed control (Figure V.1), where the fuzzy logic controller of the desired torque guarantees the convergence of the speed tracking error and imposes the desired currents computed by the PBC in Eq. (IV.9), while the damping term "K_f" in the expression of the voltage v_{dq} computed by the backstepping controller (Eqs. (V.6) and (V.7)) ensures the convergence of the current tracking error "e_{dq}" and then, the equality between the measured flux linkage ψ_{dq} and the desired ψ_{dq}^*. Therefore, the convergence of the flux linkage tracking error " $\psi_{dq} - \psi_{dq}^*$" should be ensured.

4 Adaptation of the stator resistance

Due to the designed PBC that has no direct compensation between the electrical the mechanical parts [4]. The stator resistance that appears in the expression of the control vector v_{dq} is affected by the temperature, requiring therefore to be adapted. Then, a new Lyapunov function is defined taking into account the parameter variations as follows:

$$V_s = \frac{1}{2}\left(e_d^2 + e_q^2\right) + \frac{\Delta R_s^2}{2k_s} \tag{V.8}$$

Where, $\Delta R_s = R_s - \hat{R}_s$, $\hat{R}_s$ is the estimated stator resistance and $k_s > 0$ is the adaptive gain.

The derivative of (56) yields:

$$\dot{V}_s = \dot{V} - \frac{\Delta R_s}{k_s}\dot{\hat{R}}_s \tag{V.9}$$

After calculation, we get:

$$\dot{\hat{R}}_s = k_s\left(\frac{i_d e_d}{L_d} + \frac{i_q e_q}{L_q}\right) \tag{V.10}$$

5 Simulation results and discussion

The evaluations of the proposed AFL-PBBC has been performed under MATLAB/Simulink, based on 1.5MW PMSG and 125rpm rated speed, the DC-link set value is 1150V and the reference reactive power is fixed to zero. The overall tidal conversion system parameters are listed in Table I. The initial conditions used in simulation are: the parameter $k_{f\mathrm{q}} = 100$, $[\omega_m(0), i_{dq}(0)] = [0,0,0]$ for the PMSG, Vdc(0) = 0 and $i_{daf}(0) = [0,0]$ for the grid. Using the pole placement method, the gains concerning the generator side converter controllers and the grid side current PI controller are listed in Table III. The proposed AFL-PBBC controller will be compared to FL-PBBC (the proposed method without adaptation of the stator resistance) and the conventional (PI) controller method. Two scenarios are carried out in the simulation tests, the first scenario deal with the performances of control strategies to the initial parameter values. The second scenario deal with the robustness of the proposed strategy against parameter uncertainties and disturbances. Three cases are studied in this part. In the first case, a variation of +50% of the stator resistance value R_s is performed. For the second case, a variation +100% of the total inertia J is simulated and the last test seal with the simultaneous variation of +50% R_s and +100% J.

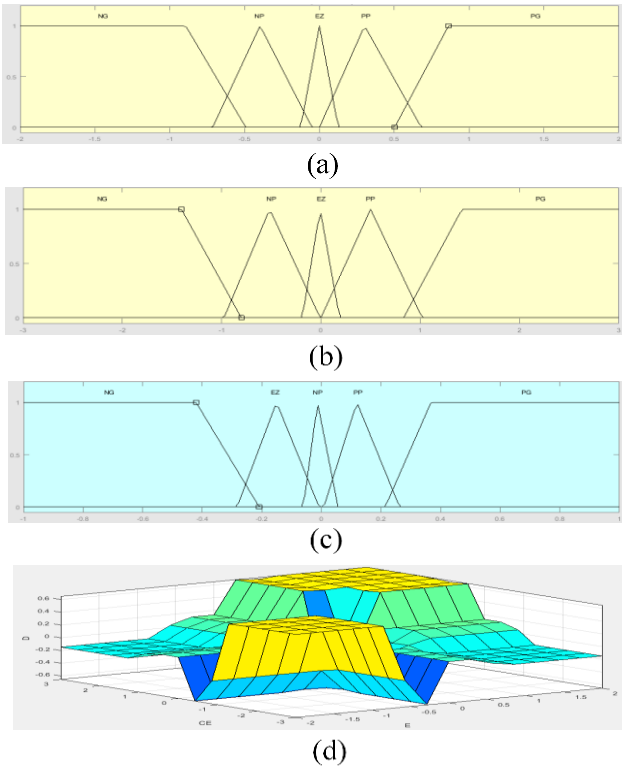

FIGURE V.2 The fuzzy controller configuration.
(a) Speed error ε_m membership function, **(b)** Variation of the speed error ε_m membership function, **(c)** Output membership function, **(d)** Control surface.

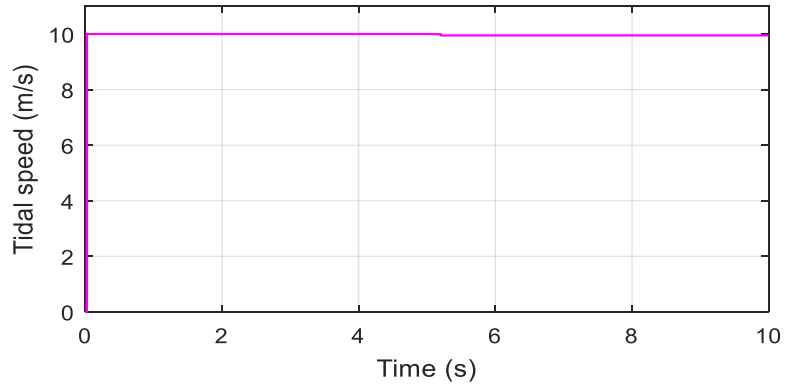

FIGURE V.3 Tidal speed.

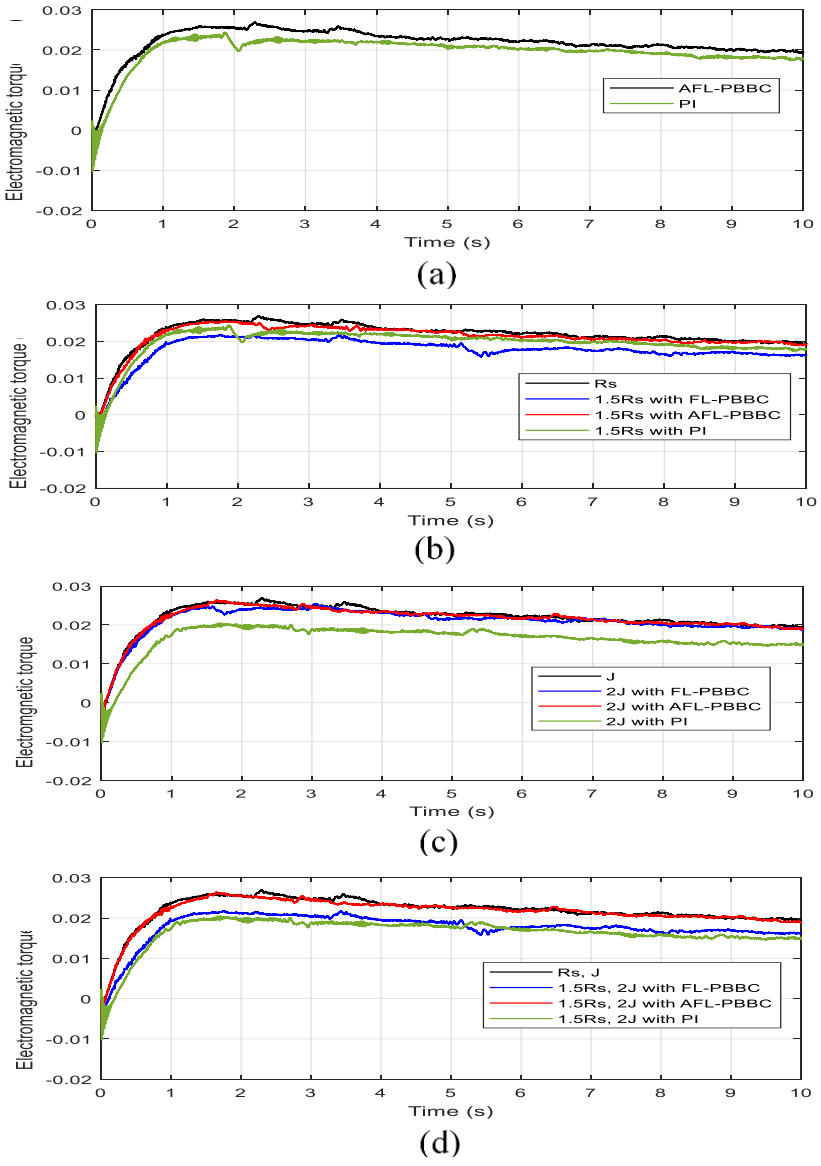

FIGURE V.4 Electromagnetic torque response in (kN.m).
(a) Initial parameters, **(b)** change +50% of R_s, **(c)** Change +100% of J, **(d)** Simultaneous change.

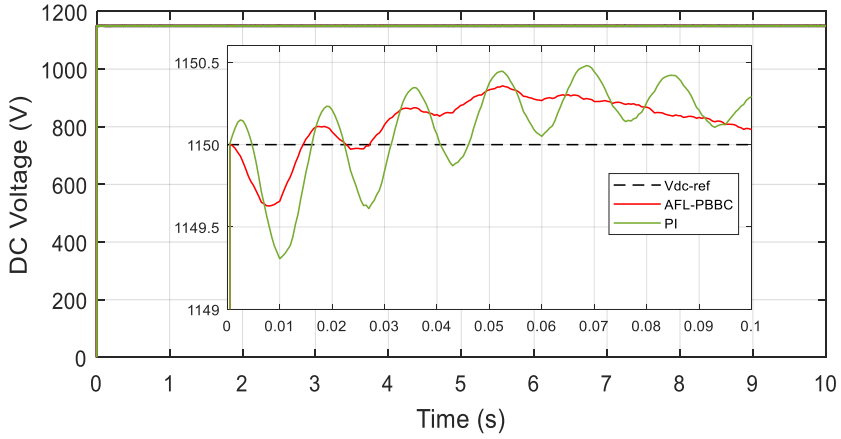

FIGURE V.5 The DC-link voltage response.

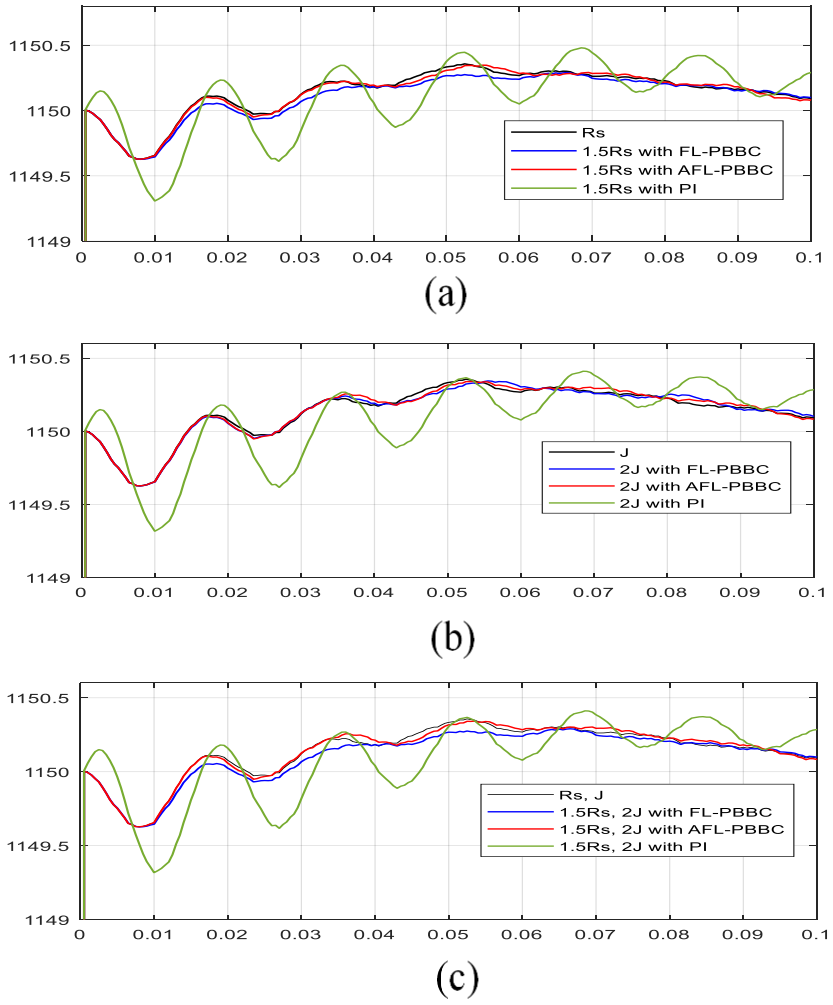

FIGURE V.6 Zoom on DC-link transitional regime.
(a) change +50% of R_s, **(b)** Change +100% of J, **(c)** Simultaneous change.

5.1 Performance analysis under fixed parameter conditions

Figure V.3, show the dynamic of the used tidal speed to test the stability of the proposed controller. Figure V.4a, show the pace of the electromagnetic torque where the established regime is stabilized, as can be seen, the proposed AFL-PBBC shows a fast convergence and a higher torque than the conventional PI control. Figure V.5 and Figure V.6a, illustrates the DC-link response, that quickly track the set value 1150V, without overshoot for the AFL-PBBC, unlike the PI strategy. Figure V.8 and Figure V.9a, shows that the reactive power quickly tracks its zero-set value, and extremely minimized for both the conventional and the proposed method. Furthermore, as can be seen, the AFL-PBBC presents a fast convergence to the zero-reference than the conventional one. In Figure V.10, as shown, the control operation achieves a perfect sinusoidal grid voltage absorption without overshoot. In this part, the proposed AFL-PBBC has successfully achieved the control objectives. The AFL-PBBC shows a higher torque, a fast convergence of the DC-link voltage and, the reactive power than the conventional PI method.

5.2 Robustness analysis

Case 1: a variation of +50% of R_s

In Figures V.4b, V.6a, V.7b, and V.9b, it can be seen that a variation of +50% of the stator resistance does not influence the dynamic of the system with the AFL-PBBC, contrary to the FL-PBBC and the conventional PI, which are sensitive to this variation. For the PI control, this is due to the fixed gains that are very sensitive to the parameter changes, concerning the FL-PBBC this is due to the backstepping controller design expressed by (V.6) and (V.7) which are influenced by R_s. Not that the linear feedback PBC is not influenced by R_s due to the imposed damping gain $k_{f\mathrm{q}}$ appearing on the PBC design in Eq. (IV.9), which compensated the variation. Because it is this gain that ensures robustness if it is chosen large compared to R_s value. As illustrated, the AFL-PBBC has remedied the disturbance of the PMSG, the DC-link voltage response, and the reactive power, quickly track their reference values.

Case 2: a variation of +100% of J

As shown in Figures. V4c, V6b, V7c, and V9c, a variation of +100% of J, has no influence on the system performance for both AFL-PBBC and FL-PBBC, this due to the fuzzy controller adopted by the PBC to design the desired torque (see Figure V.1), which has compensated the effect of J on

the mechanical part, contrary to the PI controller which is also influenced by the variation of the total moment for the same reason as mentioned in the previous case.

Case 3: simultaneous variation R_s and J

As indicated in Figures V.4d, V.6c, V.7d, and V.9d, a simultaneous variation of +50% of R_s and +100% of J, yields a same response as in the case 1 concerning the AFL-PBBC and FL-PBBC except the conventional method which is more impacted by the simultaneous variations. For the AFL-PBBC, this is due to its procedure design in section 2, 3 and 4 which compensate the parametric uncertainties as well as the convergence of the pursuit errors which are assured. Concerning the FL-PBBC response, this is due to the reasons mentioned in section 4.

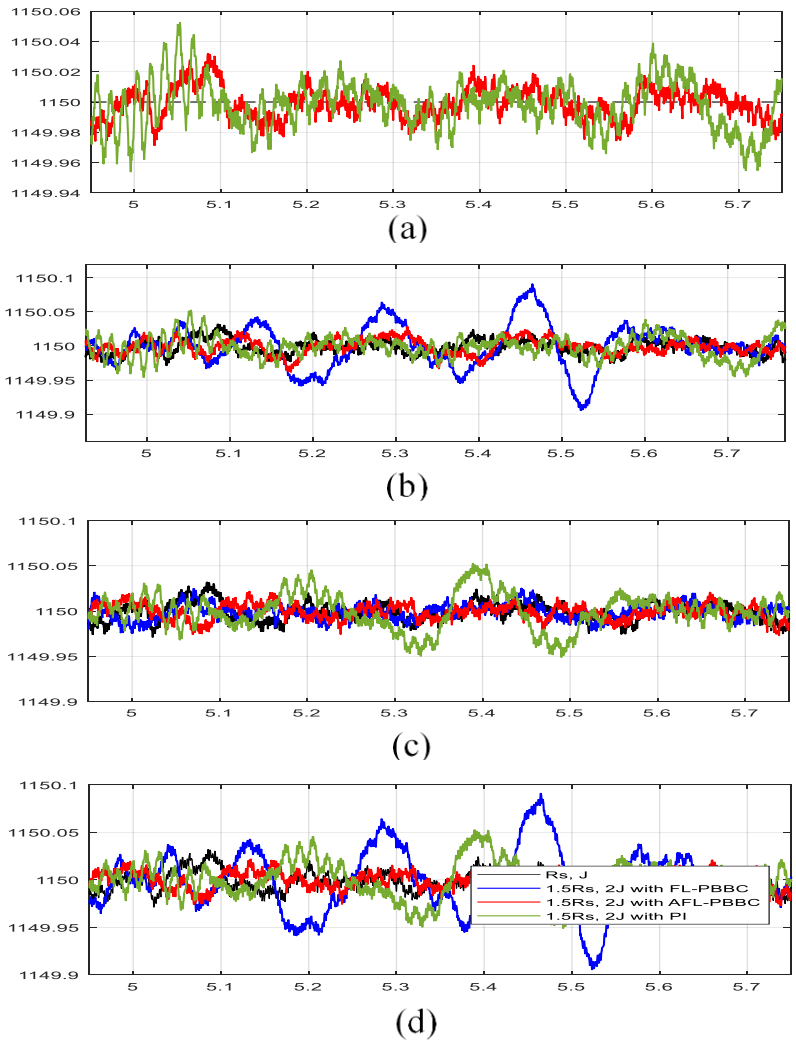

FIGURE V.7 Zoom on DC-link permanent regime.
(a) Initial parameters, **(b)** change +50% of R_s, **(c)** Change +100% of J, **(d)** Simultaneous change.

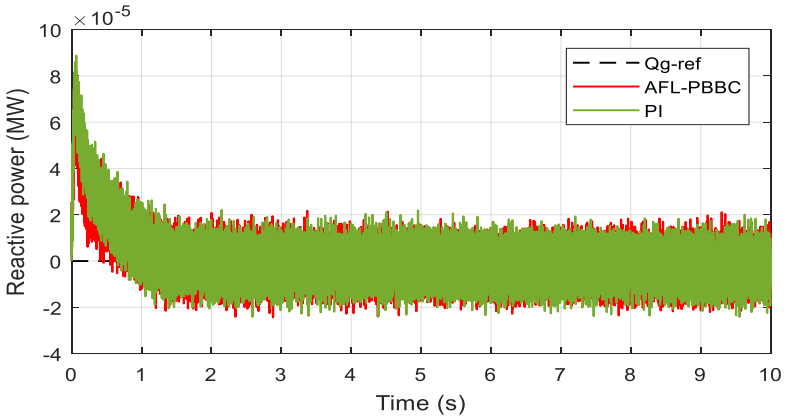

FIGURE V.8 The Reactive power.

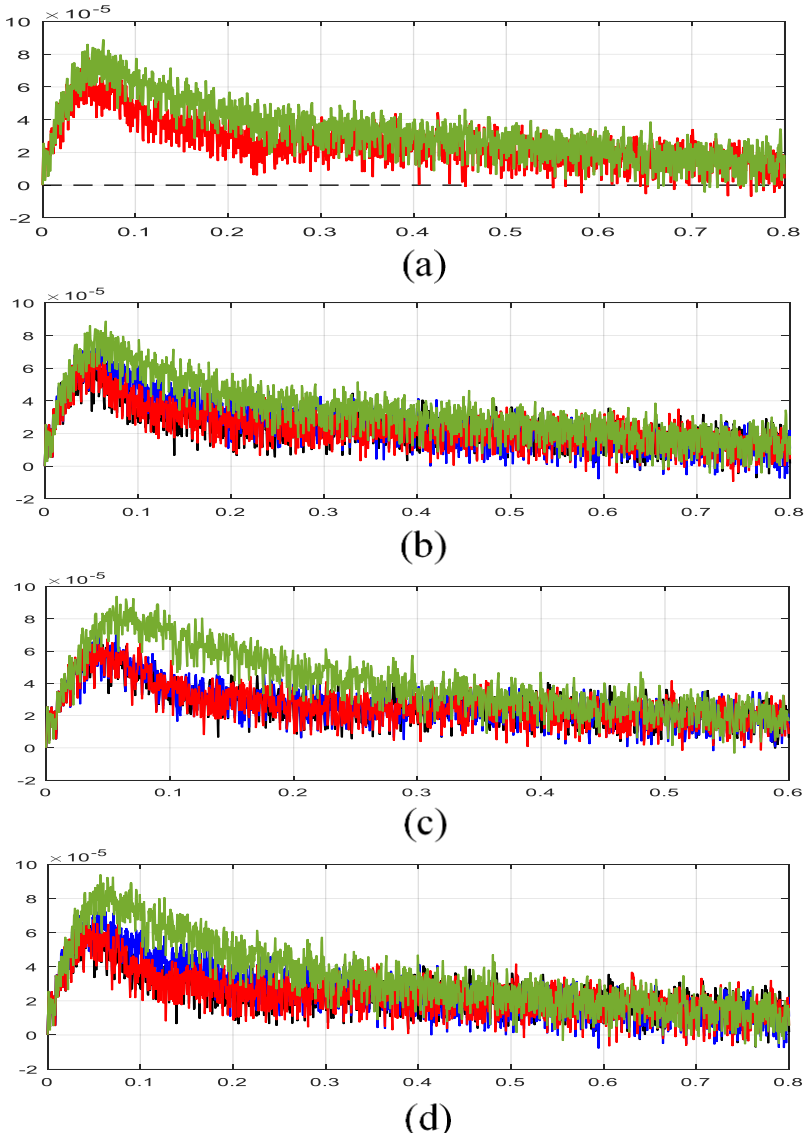

FIGURE V.9 Zoom on reactive power.
(a) Initial parameters, **(b)** change +50% of R_s, **(c)** Change +100% of J, **(d)** Simultaneous change.

5.3 Comparison

The numerical study performed in this section under the simulated tidal conversion system, demonstrate clearly that the AFL-PBBC exhibits an efficient tracking speed, higher effectiveness, it shows a fast convergence, guarantees stability, and an extremely robustness performance against parameter changes compared to conventional approaches, such as second-order sliding mode control [5] and PI-control [6], considering the nonlinear model of the system.

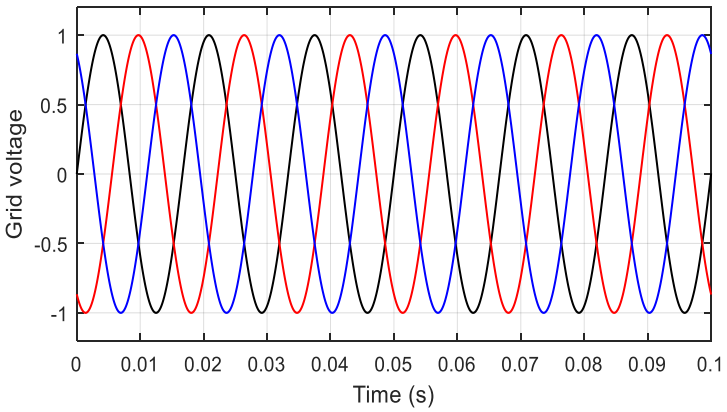

FIGURE V.10 Voltage transmitted to the grid (pu).

6 Conclusion

A new control strategy for a tidal turbine-based PMSG conversion system is developed. The modeling and the methodology for the adaptive fuzzy linear feedback passivity-based backstepping control of the PMSG have been described. The simulation results performed using MATLAB/Simulink environment with the inclusion of the dynamics of the PMSG for a used tidal speed, show the effectiveness of the conversion system. The proposed method, shows the fast-tracking of the maximum tidal power point, the DC-link and the reactive power generated are very well kept at their constant values with an extremely minimized error. The control strategy exhibits higher torque, an efficient tracking speed, higher effectiveness, and an extremely robustness performance against parameter changes compared to the conventional controller. Then, the tidal conversion system-based PMSG provides good performance, efficiency, and significant robustness against generator parameter uncertainties. The control strategy has a simple structure, is reasonable, and is highly promising in tidal energy applications.

References

[1] Achour AY, Mendil B, Bacha S, Munteanu I. Passivity-based current controller design for a permanent-magnet synchronous motor. ISA Transactions, 2009; 48(3): 336-346.

[2] Belkhier Y, Achour AY. Passivity-based voltage controller for tidal energy conversion system with permanent magnet synchronous generator. International Journal of Control, Automation and Systems, 2020; 19: 1-11.

[3] Belkhier Y, Achour AY. An intelligent passivity-based backstepping approach for optimal control for grid-connecting permanent magnet synchronous generator-based tidal conversion system. Int. J. Energy Res., 2020: 1-16. DOI: 10.1002/er.6171.

[4] Wang J, Bo D, Ma X, Zhang Y, Li Z, Miao Q. Adaptive back-stepping control for a permanent magnet synchronous generator wind energy conversion system. international journal of hydrogen energy, 2019; 44(5): 3240-3249.

[5] Mousa HHH, Youcef AR, Mohamed EEM. Variable step size P&O MPPT algorithm for optimal power extraction of multi-phase PMSG based wind generation system. Electrical Power and Energy Systems, 2019; 108: 218-231.

[6] Zhou Z, Scuiller F, Charpentier JF, Benbouzid MEH, Tang T. Power smoothing control in a grid-connected marine current turbine system for compensating swell effect. IEEE Transaction on Sustainable Energy, 2013; 4(3): 816-826.

Conclusions

This PhD thesis has focused on some important challenges in tidal turbine systems. Firstly, up-to-date information on tidal current turbine technologies and demonstrative farm projects has been presented. Therefore, a review of energy storage system technologies has been carried out in the first chapter and also the deferents configuration of the tidal conversion system investigated in the literature and the industry. Moreover, a review on passivity-based control has been investigated and updated. The problematic concerning this thesis has also been illustrated. This thesis has proposed three deferents controller to overcome the problematic. The main conclusions are listed as follows:

- The era of megawatt-level tidal conversion system has arrived. Concerning the identified problemes in marine current-based PMSG generation systems, hybrid energy storage systems should be considered to improve the system power performance.
- In tidal conversion system the mechanical parameters of the PMSG causes numerous problems. In this case, a pasivitity-based voltage controller has been proposed. The simulation results have clearly shown the effectiveness of the proposed control strategy.
- A second controller is proposed also, this time a passivity-based current controller combined with a fuzzy logic controller and a linear feedback controller is investigated. The simulation results have clearly shown the effectiveness of the proposed control strategy.
- For over-rated current speed and parameter uncertainties, a robust passivity controller is developed, the proposed controller combined the proposed one in the chapter three with a backstepping controller which has improved considerably the proposed one in the chapter three. Also, an adaptation of the stator resistance has been adopted to guarantee the robustness of the controller. The simulation results show that this adaptive control strategy is more effectiveness than the two other strategies proposed in this thesis.

The perspectives following the above development can be mainly divided into two aspects: fault tolerant control strategies and turbine farm simulations. Indeed, some improvements should be considered in future works: Include fault-tolerant control strategies. For a grid-connected system, how to maintain a stable operation in case of grid faults (low voltage ride through, frequency distortion) is very important. Extend the single tidal conversion system case of this thesis to a MCT farm study.

Appendix

1 Appendix A

proof of the currents error exponential stability

Considering Eq. (III.3), which by the Rayleigh quotient and the matrix $L_{\alpha\beta}$ positivity, guarantees the following inequality:

$$0 \leq \lambda_{\min}\{L_{\alpha\beta}\}\|\varepsilon_i\|^2 \leq V_f^*(\varepsilon_i) \leq \lambda_{\max}\{L_{\alpha\beta}\}\|\varepsilon_i\|^2 \tag{A.1}$$

Where, $\lambda_{\max}\{L_{\alpha\beta}\}$ and $\lambda_{\min}\{L_{\alpha\beta}\}$ are the matrix $L_{\alpha\beta}$ maximum and the minimum eigenvalues.

The time derivative of (III.3) along (III.4) and (III.5), which by the Rayleigh quotient and the dissipation term $R_{\alpha\beta} + B_i$ positivity, guarantees the following inequality:

$$V_f^*(\varepsilon_i) = -\varepsilon_i^T\left(R_{\alpha\beta} + B_i\right)\varepsilon_i \leq -\lambda_{\min}\{R_{\alpha\beta} + B_i\}\|\varepsilon_i\|^2, \forall t \geq 0 \tag{A.2}$$

Where, $\lambda_{\min}\{R_{\alpha\beta} + B_i\} > 0$ represents the matrix $R_{\alpha\beta} + B_i$ minimum eigenvalue.

From (A.1) and (A.2), we deduce the following inequality:

$$\dot{V}_f^*(\varepsilon_i) = -r_1 V_f^*(\varepsilon_i) \tag{A.3}$$

Where, $r_1 = \frac{\lambda_{\min}\{R_{\alpha\beta}+B_e\}}{\lambda_{\max}\{L_{\alpha\beta}\}} > 0$.

By integrating (A.3), we obtain the following inequality:

$$\dot{V}_f^*(\varepsilon_i) \leq V_f^*(0)e^{-r_1 t} \tag{A.4}$$

From (A.1) ad (A.4), we get:

$$\|\varepsilon_i\| \leq r_2\|\varepsilon_i\|e^{-r_1 t} \tag{A.5}$$

Where, $r_2 = \sqrt{\frac{\lambda_{\min}\{L_{\alpha\beta}\}}{\lambda_{\mathrm{mix}}\{L_{\alpha\beta}\}}} > 0$.

Therefore, the current tracking error is exponentially decreasing with a rate of convergence r_1.

2 Appendix B

The System parameters used in the simulation:

Table 2. System parameters

PMSG PARAMETER	Value
Tidal turbine radius (R)	10 m
Water density (ρ)	1024 kg/m^3
Stator resistance (R_s)	0.006 ^{R_s}
Stator inductance ($L_d = L_q$)	0.3 mH
Pole pairs number (p)	48
Flux linkage (ϕ_f)	1.48 Wb
Total inertia (J)	35000 kg.m^2
DC-link voltage (V_{dc})	1150 V
DC-link capacitor (C)	2.9 µF
Grid voltage (V_g)	574 V
Grid-filter resistance (R_f)	0.3 pu
Grid-filter inductance (L_f)	0.3 pu

ABSTRACT: This PhD thesis models the whole power chain of a tidal current turbine system and investigates the use of passivity-based control strategy to improve power quality. First, a passivity-based voltage control method is proposed to address the problems faced by the conventional PI controls in the machine-side of the tidal current generation system. Second, a passivity-based current control combined with fuzzy logic strategy is investigated. The proposed control strategy uses a PI loops to design the control law and the desired torque on the generator-side. Finally, a passivity-based backstepping control and fuzzy logic control is proposed. In this context, the backstepping strategy is selected to improve speed tracking error convergence, while the fuzzy logic controller is introduced to design the desired torque and introducing more robustness properties over the nonlinear dynamical and time-varying parameters of the closed-loop system. in the present work, the tidal conversion system is connected to the grid, thus, a classical PI control is adopted for the grid-side converter, for injecting a smoothed power to the grid.

RESUME : ces travaux de thèse concernent l'étude d'une chaine de conversion d'énergie hydrolienne connecté aux réseaux électrique. L'objectif principale est de maximiser l'énergie extraite du courant marin et de résoudre les problèmes liés au variation paramétriques ainsi que les propriétés non linéaires du system de conversion en utilisant la commande basée sur la passivité (CBP). Une CBP commandée en tension est proposée pour résoudre les problèmes de robustesses rencontré par les commandes classique dans le coté génératrice. Ensuite, une CBP commandée en courant associée à la commande floue est développé. Enfin, une CBP associée à la commande de backstepping et de la commande floue est proposé. Pour cette dernière, le backstepping est utilisé pour améliorer le temps de réponse, et la commande flou est sélectionné pour améliorer la robustesse du system. La méthode vectorielle classique est utiliser pour injecter la puissance électrique produite par la génératrice dans le réseau électrique.

ملخص

تقوم أطروحة الدكتوراه هذه بوضع نماذج لسلسلة الطاقة الكاملة لنظام توربينات تيار المد والجزر وتحقق في استخدام استراتيجية التحكم القائمة على السلبية لتحسين نوعية الطاقة. فأولا ، يُقترح اتباع طريقة للتحكم في الفولتية قائمة على السلبية لمعالجة المشاكل التي تواجهها أجهزة التحكم التقليدية في نظام توليد تيار المد والجزر. وثانيا ، يجري التحقيق في السيطرة الحالية القائمة على السلبية مقترنة باستراتيجية منطقية غامضة. وتستخدم استراتيجية التحكم المقترحة حلقات برمجية لتصميم قانون التحكم والعزم المرغوب على جانب المولد. وأخيرا ، يُقترح فرض رقابة على الدعم القائم على السلبية والتحكم في المنطق الغامض وفي هذا السياق ، يتم اختيار استراتيجية الدعم لتحسين تقارب الأخطاء في تتبع السرعة ، في حين يتم إدخال جهاز التحكم المنطقي الغامض لتصميم الدوران المرغوب فيه وإدخال خصائص أكثر قوة على البارامترات غير الديناميكية والمتغيرة زمنيا لنظام الحلقة المغلقة. وفي العمل الحالي ، يرتبط نظام تحويل المد والجزر بالشبكة ، ومن ثم ، يتم اعتماد نظام رقابة كلاسيكي من أجل محول جانب الشبكة ، لحقن طاقة سلسة بالشبكة..